

## V. THEORETICAL PHYSICS

### OVERVIEW

Research in the Physics Division's Theory Group addresses a broad range of important problems involving the structure and dynamics of hadrons and nuclei. There is a strong emphasis on comparison with data from Argonne's ATLAS facility, from TJNAF, and from other laboratories around the world. Our work includes the modeling and application of quantum chromodynamics (QCD) to light- and heavy-hadron structure at zero temperature and density, and at the extremes of temperature and density appropriate to the early universe, neutron stars, and RHIC experiments. We develop reaction theories to use in exploring hadron structure using the data from meson and nucleon-resonance production experiments at TJNAF, MIT-Bates and Mainz. We construct realistic two- and three-nucleon potentials that give accurate fits to nucleon-nucleon elastic scattering data and trinucleon properties, and use them in detailed many-body calculations of light and near closed-shell nuclei, nuclear matter and neutron stars, and in a variety of astrophysically important electroweak reactions. Our nuclear structure and reaction studies include coupled-channels calculations of heavy-ion reactions near the Coulomb barrier and calculations of observables in breakup reactions of nuclei far from stability. We also study high-spin superdeformation, spectroscopy of the heaviest elements ( $A \geq 250$ ), and nuclear structure near the proton-drip line. Additional research is pursued in atomic physics, neutron physics, quantum computing, and fundamental quantum mechanics. Several of our projects involve major numerical simulations using the massively parallel computer systems at Argonne and NERSC.

### A. NUCLEAR DYNAMICS WITH SUBNUCLEONIC DEGREES OF FREEDOM

The objective of this research program is to investigate the role of: quark-gluon degrees of freedom in hadron structure and interactions, and in nuclear dynamics; the development and application of reaction theories for use in exploring hadron structure using the data from meson and nucleon-resonance production experiments at modern experimental facilities; and to investigate relations of Poincaré covariant dynamics specified by mass operators to complementary dynamics specified by Green functions.

At the level of quark-gluon degrees of freedom, the Dyson-Schwinger equations (DSEs) provide a Poincaré covariant, nonperturbative method for studying QCD in the continuum. The existence of symmetry preserving truncations enables the simultaneous exploration of phenomena such as: confinement, dynamical chiral symmetry breaking, and bound state structure and interactions. In addition the DSEs provide a generating tool for perturbation theory and hence yield model-independent results for the ultraviolet behavior of strong interaction observables. This means that model studies facilitate the use of physical processes to constrain the long-range behavior of the quark-quark interaction in QCD, which is poorly understood and whose elucidation is a key goal of modern experimental programs. The last year has seen many successful applications. For example, we solved a Faddeev equation for the nucleon and Delta and showed that a description in terms of confined-quark and nonpoint-like confined-diquark-correlations can readily be obtained. We found in addition that the self-energy contribution from the  $\pi N$  loop can reduce the nucleon's mass by up to several hundred MeV. We saw, however, that this effect does not qualitatively alter the picture that baryons are quark-diquark composites. And, using a Vlasov equation coupled to Maxwell's equation, we showed that focused laser beams at proposed X-ray free electron laser facilities can generate electric field strengths large enough to cause spontaneous electron-positron pair production from the QED vacuum. Our study predicts the production of a few hundred particle pairs per laser period and hence that an experimental verification of vacuum decay is within reach.

At the level of meson and baryon degrees of freedom, we have developed a dynamical model for interpreting  $\gamma N$  reactions in terms of the quark-gluon substructure of nucleon resonances ( $N^*$ ) as predicted by various QCD-based hadron models. In the past year the model has been instrumental in quantifying the pion cloud contribution to the  $Q^2$ -dependence of the  $\gamma N \rightarrow \Delta$  transition factors, extracted from the recent data obtained at TJNAF, Mainz, MIT-Bates and NIKHEF. We have also used the model to make predictions for the  $d(e, e'\pi)$  reaction and  $\eta$  production in NN collisions, with an aim of using the new data from TJNAF and COSY to investigate the medium effects on meson and  $N^*$  propagation. Our investigation of vector meson photoproduction has been extended to consider coupled-channel effects and include the sub-threshold  $N^*$  excitations. Finally, we have provided theoretical guidance for designing experiments to use various spin observables in  $\pi$  photoproduction to resolve the "missing" resonance problem.

Relativistic quantum dynamics requires a unitary representation of space-time symmetries (Poincaré group) and localization of states, such that states localized in relatively space-like regions are causally independent. For finite systems Poincaré generators obtain as functions of mass and spin operators. With realistic restrictions of the mass operator the dynamics is "almost

local” as defined precisely in the context of algebraic quantum field theory. The fundamental limitation to finite systems may be overcome by the relation to relativistic dynamics specified by Green operators with the required spectral properties.

### a.1. Contemporary Applications of Dyson-Schwinger Equations (M. B. Hecht, C. D. Roberts and S. M. Schmidt)

The contemporary application of DSEs is well illustrated by the calculation of pseudoscalar meson masses and the study of nucleon observables. For the former, we showed that a direct solution of the appropriate Bethe-Salpeter equations, combined with the knowledge provided by a DSE-derived model-independent mass-formula, predicts the current-quark-mass-dependence of pseudoscalar meson masses recently measured in lattice-QCD simulations. Importantly our analysis also provides an intuitive

understanding, relating the evolution to a large value of the vacuum and in-hadron quark condensates. For the latter, we showed that a Poincaré covariant Faddeev equation, which describes a baryon as a composite of a dressed quark and nonpoint-like, dressed scalar and axial-vector diquarks, provides an internally consistent picture of the nucleon and  $\Delta$ . An article describing these results was published.<sup>1</sup>

<sup>1</sup>M.B. Hecht, C.D. Roberts and S.M. Schmidt, *Contemporary Applications of Dyson-Schwinger Equations*, in "Quark Confinement and the Hadron Spectrum IV," edited by W. Lucha and Kh. Maung-Maung (World Scientific, Singapore, 2002) pp. 27-39

### a.2. Diquarks and Density (M. B. Hecht, C. D. Roberts, and S. M. Schmidt)

A diquark is a bosonic quark-quark correlation, which is necessarily colored in all but 2-color QCD (QC<sub>2</sub>D). Therefore, in the presence of color-confinement, diquarks cannot be directly observed in a 3-color gauge theory's spectrum. Nevertheless, evidence is accumulating; *e.g.*, via Faddeev equation studies, which suggests that confined diquark correlations play an important role in hadronic spectroscopy and interactions. The significance of diquarks in those applications motivates a study of the possibility that dense hadronic matter may exhibit diquark condensation; *i.e.*, quark-quark pairing promoted by a quark chemical potential. To explore this we introduced a Gorkov-Nambu-like gap equation for QCD and applied it to QC<sub>2</sub>D and, in two

qualitatively different truncations, to QCD itself. Among other interesting features, we demonstrated that QC<sub>2</sub>D with massive fermions undergoes a second-order transition to a superfluid phase when the chemical potential exceeds  $m_\pi/2$ . In the QCD application we illustrated that the  $\sigma := -\langle \bar{q}q \rangle^{1/3} \neq 0$  phase, which determines the properties of the strong-interaction's mass spectrum at zero temperature and chemical potential, is unstable with respect to the superfluid phase when the chemical potential exceeds  $\sim 2\sigma$ , and that at this point the diquark gap is large,  $\sim \sigma/2$ . This superfluid phase survives to temperatures greater than that expected in the core of compact stars. An article describing this work was published.<sup>1</sup>

<sup>1</sup>M.B. Hecht, C. D. Roberts and S. M. Schmidt, *Diquarks and Density*, in "Physics of Neutron Star Interiors," edited by D. Blaschke, N. K. Glendenning and A. Sedrakian (Springer Publishing, Berlin Heidelberg, 2001) pp. 218-234

### a.3. Pair Creation and Plasma Oscillations (S. M. Schmidt, M. B. Hecht, C. D. Roberts, A. V. Prozorkevich,\* and D. V. Vinnik\*)

Ultra-relativistic heavy-ion collisions (URHICs) are complicated processes and their understanding requires a microscopic modeling of all stages: the formation, evolution and hadronization of a strongly coupled plasma. With RHIC now operating it is imperative to develop a microscopic understanding of URHICs, including their non-equilibrium aspects. In response to this challenge we studied particle creation in strong fields in the presence of thermalizing collisions. Our quantum kinetic equation involved a non-Markovian source term and a relaxation time approximation to the collision term, and the strong electric background field

was determined by coupling-in Maxwell's equation and solving the whole system self-consistently. Plasma oscillations are an almost inevitable outcome of this treatment. We found that the plasma frequency depends on at least three quantities: the field strength, the relaxation time and the mass distribution of the produced particles. In addition, we observed that incorporating a strongly momentum-dependent dressed-parton mass, which is an essential feature of QCD, can have a significant impact on the evolution of the plasma. In particular it promotes plasma oscillations. An article describing this work was published.<sup>1</sup>

\*Saratov State University, Armenia

<sup>1</sup>A. V. Prozorkevich, D. V. Vinnik, S. M. Schmidt, M. B. Hecht, and C. D. Roberts, *Pair Creation and Plasma Oscillations*, in "Quark Matter in Astro- and Particle-physics," edited by G. R. G. Burau, D. B. Blaschke and S. M. Schmidt (Rostock University Press, Rostock, 2001) pp. 79-88

### a.4. Neutron Electric Dipole Moment: Constituent-Dressing and Compositeness (M. B. Hecht, C. D. Roberts, and S. M. Schmidt\*)

The action for any local quantum field theory is invariant under the transformation generated by the antiunitary operator CPT, which is the product of the inversions: C - charge conjugation; P - parity transformation; and T - time reversal. The decay of the CP-odd eigenstate  $K_0^L$  into a CP-even  $2\pi$  final state demonstrates that the product of only C and P is not a good symmetry of the standard model. This entails that time reversal invariance must also be violated and that, too, has been observed in detailed studies of the neutral kaon system. It has long been known that the possession of an electric dipole moment (EDM) by a spin-1/2 particle would signal the violation of time-reversal invariance. (The existence of a dipole moment signals a spherically asymmetric distribution of charge.) Any such effect is likely small, given the observed magnitude of CP and T violation in the neutral kaon system, and this makes neutral particles the obvious subject for experiments: the existence of an electric monopole charge would overwhelm most signals of the dipole strength. It is therefore natural to focus on the neutron, which is the simplest spin-1/2 neutral composite system in nature. Attempts to measure the

neutron's EDM,  $d_n$ , have a long history and currently yield the upper bound:

$$d_n < 6.3 \times 10^{-26} \text{ e cm (90\% CL).}$$

This has proven to be an effective constraint on attempts to extend the standard model and to assist in this we have calculated  $d_n$  using a well-constrained Ansatz for the nucleon's Poincaré covariant Faddeev amplitude. We found that the momentum-dependent quark dressing amplifies the contribution from the current-quarks' EDMs; and that dressed-quark confinement and binding make distinguishable the effect of the two CP and T violating interactions:  $i\gamma_5\sigma_{\mu\nu}(p_1-p_2)_\nu$  and  $\gamma_5(p_1+p_2)_\mu$ , where  $p_{1,2}$  are the current-quarks' momenta. In addition, our calculation showed that the value of  $|d_n|$  obtained using the current-quark EDMs generated by a minimal three Higgs doublet model of spontaneous CP violation is perilously close to the experimental upper bound; *i.e.*, that the so-called Weinberg model is almost excluded by this bound. An article describing our work was published.<sup>1</sup>

\*University of Tuebingen, Germany

<sup>1</sup>M. B. Hecht, C. D. Roberts, and S. M. Schmidt, Phys. Rev. C **64**, 025204 (2001)

**a.5. Plasma Production and Thermalization in a Strong Field** (M. B. Hecht, C. D. Roberts, S. M. Schmidt,\* D. V. Vinnik,\* A. V. Prozorkevich,† S. A. Smolyansky,‡ and V. Toneev‡)

We have extended and improved the collision term in our quantum Vlasov equation, and reanalyzed aspects of the formation and equilibration of a quark-gluon plasma. In addition, since leptons do not participate in the strong interactions that equilibrate the QGP, we calculated the thermal dilepton spectrum produced by the evolving plasma. We again found that field-current feedback generates plasma oscillations in all thermodynamic observables. The oscillations were also evident in the production rate of thermal dileptons.

While the time evolution of that rate may not be measurable, the plasma oscillations also acted to significantly enhance the time-integrated rate, which is easily accessible. This effect was marked by a sharp increase in the dilepton yield once the energy-density-per-parton became large enough to generate a high frequency and large amplitude plasma oscillation, which could survive the effect of damping for a significant time after the moment of impact. An article describing this work was published.

\*University of Tuebingen, Germany, †Saratov State University, Armenia, ‡BLTP, JINR, Dubna

<sup>1</sup>D. V. Vinnik, A. V. Prozorkevich, S. A. Smolyansky, V. D. Toneev, M. B. Hecht, C. D. Roberts, and S. M. Schmidt, Eur. Phys. J. C **22**, 341 (2001)

**a.6. Meson Photoproduction** (M. B. Hecht, C. D. Roberts, and S. M. Schmidt\*)

The dichotomy of the pion as QCD's Goldstone mode and a bound state of massive constituents is easily understood using the Dyson-Schwinger equations. That provides the foundation for an efficacious phenomenology, which correlates the pion's charge radius and electromagnetic form factor with its valence quark distribution function; and simultaneously provides a Poincaré covariant description of the nucleon, its form factors and, more recently, meson photoproduction processes. The latter processes are important for developing an understanding of the structure of nucleon resonances and in searching for "missing" resonances; *i.e.*, those states predicted by constituent quark models that are hitherto unobserved. Preliminary parameter-free calculations of the t-channel pion-exchange contribution to the  $\omega$ -photoproduction cross-section

reproduce the forward angle cross-section exactly, as illustrated in Fig. V-1. A comparison between the results in this approach and experiment at large-angles is meaningless until the contribution of the s- and u-channel processes are also included, a calculation that is underway. The analogous t-channel contribution to pion photoproduction has also been calculated and the results justify, a posteriori, the meson-exchange model expedient of neglecting quark-gluon substructure in the photon-pion vertex. The role of substructure in the meson-nucleon vertices is more important and such parameter-free calculations will facilitate the qualitative improvement of meson exchange models by making possible the explicit representation of these effects. Articles describing this work have been or will be published.<sup>1,2</sup>

\*University of Tuebingen, Germany

<sup>1</sup>M. B. Hecht, C. D. Roberts and S. M. Schmidt, *The Character of Goldstone Bosons*, in "Lepton-Scattering, Hadrons and QCD," edited by W. Melnitchouk, A. W. Schreiber, A. W. Thomas and P. C. Tandy (World Scientific, Singapore, 2001) pp. 219-227

<sup>2</sup>M. B. Hecht and C. D. Roberts, *Modern Dyson-Schwinger Equation Studies*, to appear in the "πN Newsletter"

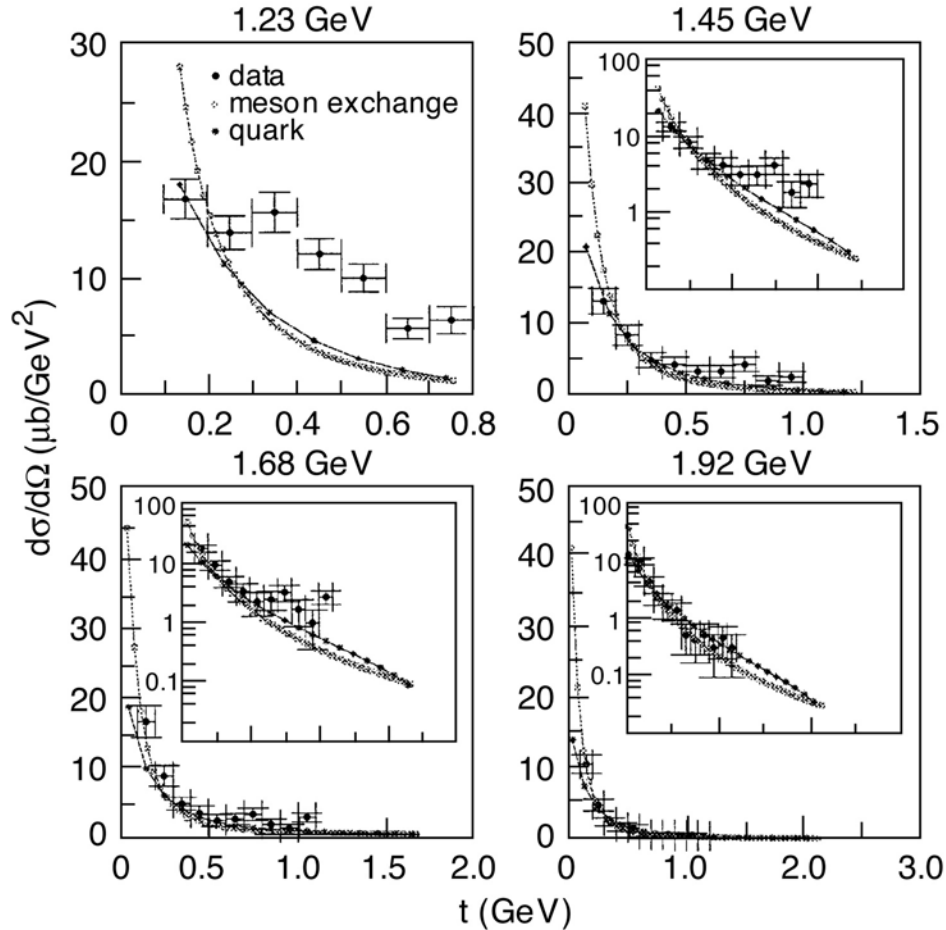


Fig.V-1.  $\pi$ -exchange contribution to the  $\gamma N \rightarrow \omega N$  cross section obtained using the model of Hecht, Roberts, and Schmidt [Phys. Rev. C **64**, 025204 (2001)]. (Panels are labeled by the incident photon energy.) \*, long-dashed line, our calculation (no parameters were varied to obtain this result); , short-dashed line, the meson-exchange model calculation of Oh, Tito, and Lee [Phys. Rev. C **63**, 025201 (2001)] (only the  $t$ -channel  $\pi$ -exchange contribution is shown); data from Klein et al. [Saphir Collaboration,  $\pi N$  Newsletter **14**, 141 (1998).]

#### a.7. Pair Creation and an X-ray Free Electron Laser (M. B. Hecht, C. D. Roberts, R. Alkofer,\* S. M. Schmidt,\* and D. V. Vinnik\*)

Using a quantum kinetic equation coupled to Maxwell's equation we studied the possibility that focused beams at proposed X-ray free electron laser facilities can generate electric field strengths large enough to cause spontaneous electron-positron pair production from the QED vacuum; *i.e.*, to cause the "decay of the vacuum." We calculated the time and momentum dependence of the single particle distribution function, and established that field-current feedback and quantum statistical effects are small and can be neglected in this

application of non-equilibrium quantum mean field theory. We found that, under conditions reckoned achievable at planned facilities, repeated cycles of particle creation and annihilation take place in tune with the laser frequency. However, the peak particle number density is insensitive to this frequency, as evident in Fig. V-2, and hence we predict the production of a few hundred particle pairs per laser period. This means that an experimental verification of vacuum decay is within reach. An article describing this work was published.<sup>1</sup>

\*University of Tuebingen, Germany

<sup>1</sup>R. Alkofer, M. B. Hecht, C. D. Roberts, S. M. Schmidt, and D. V. Vinnik, Phys. Rev. Lett. **87**, 193902 (2001)

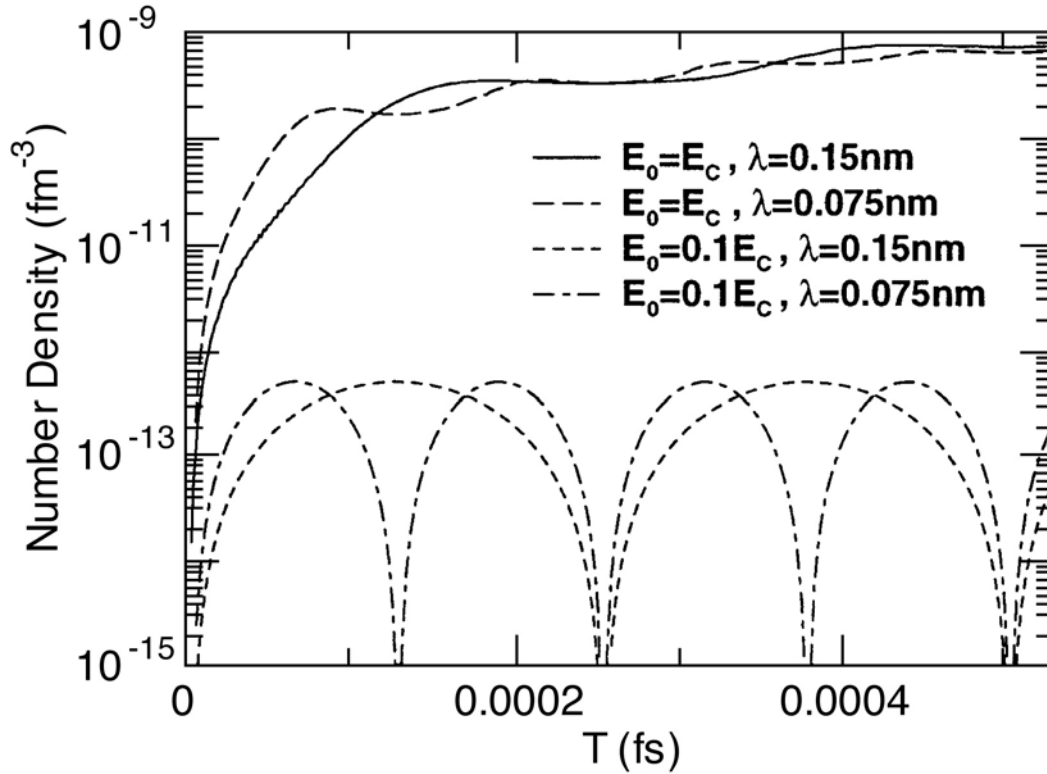


Fig.V-2. Time evolution of the particle number density for the XFEL design-goal field strength:  $E = 0.1 E_{cr}$ , and for strong fields:  $E = E_{cr}$  [ $E_{cr} = m_e^2/e = 1.3 \times 10^{18}$  V/m.]. In strong fields, particles accumulate, leading to the almost complete occupation of available momentum states. In weak fields, repeated cycles of particle creation and annihilation occur in tune with the laser frequency. We estimate that hundreds of particles will be produced in each cycle.

#### a.8. X-ray Free Electron Laser: Vacuum Pair Creation, Back Reactions and Memory Effects (C. D. Roberts, S. M. Schmidt,\* and D. V. Vinnik\*)

Spontaneous electron-positron pair production out of the QED vacuum is possible in the presence of homogeneous electric fields with a strength characterized by  $e E_{cr} = m_e^2$ . X-ray free electron laser (XFEL) facilities planned at DESY and SLAC will achieve fields  $E \sim 0.1 E_{cr}$  and make vacuum decay observable but will not lead to an accumulation of particles (see Fig.V-2). We have applied our quantum kinetic approach and found that particle accumulation is likely to occur at fields  $E \sim 0.25 E_{cr}$ . We found, too, that with accumulation non-Markovian features in the particle source term become observable; i.e., the time between production events becomes commensurate

with the produced parton's Compton frequency and hence interference effects become apparent that expose the negative energy elements in the particle wave packets. This is a core quantum field theoretical feature. At larger field strengths:  $E \sim 0.5 E_{cr}$ , the accumulating system of partons will exhibit plasma oscillations. This study suggests that a greater body of fundamental phenomena will be accessible at XFEL facilities if the design goals can be modestly exceeded. It was possible only because we have developed and directly applied a quantum Vlasov equation. We are preparing an article that describes this research.

\*University of Tuebingen, Germany

**a.9. Nucleon Mass and Pion Loops** (M. B. Hecht, C. D. Roberts, A. W. Thomas,\*  
M. Oettel,\* S. M. Schmidt,† and P. C. Tandy‡)

We solved Poincaré covariant Faddeev equations for the nucleon and  $\Delta$  to illustrate that an internally consistent description in terms of confined-quark and nonpoint-like confined-diquark-correlations can readily be obtained. Subsequently, we calculated the  $\pi$ N-loop induced self-energy corrections to the nucleon's mass and showed them to be independent of whether a pseudoscalar or pseudovector coupling is used. Applying phenomenological constraints, we argued that

this self-energy correction reduces the nucleon's mass by up to several hundred MeV. However, we demonstrated that this effect does not qualitatively alter the picture, suggested by the Faddeev equation, that baryons are quark-diquark composites, although neglecting the  $\pi$ -loops leads to a quantitative overestimate of the nucleon's axial-vector diquark component. An article describing this work was accepted for publication.

\*CSSM, University of Adelaide, Australia, †University of Tuebingen, Germany, ‡Kent State University

**a.10. Bethe-Salpeter Equation and a Nonperturbative Quark-gluon Vertex**  
(C. D. Roberts, A. Bender,\* W. Detmold,\* and A.W. Thomas\*)

A Ward-Takahashi identity preserving Bethe-Salpeter kernel can always be calculated explicitly from a dressed-quark-gluon vertex whose diagrammatic content is enumerable. We illustrated that fact using a vertex obtained via the complete resummation of dressed-gluon ladders. While this vertex is planar, the vertex-consistent kernel is nonplanar and that is true for any dressed vertex. In an exemplifying model, the rainbow-ladder truncation of the gap and Bethe-Salpeter equations yielded many results; *e.g.*,  $\pi$ - and  $\rho$ -

meson masses, that are changed little by including higher-order corrections. However, repulsion generated by nonplanar diagrams in the vertex-consistent Bethe-Salpeter kernel for quark-quark scattering is sufficient to guarantee that diquark bound states do not exist. This analysis confirms the importance of preserving symmetries in studies of QCD's bound states. An article describing this work was submitted for publication.

\*CSSM, University of Adelaide, Australia

**a.11. Axial-Vector Diquarks in the Baryon** (C. D. Roberts)

It has been shown that a product Ansatz for the nucleon's Faddeev amplitude using only a scalar-diquark can provide a good description of leptonic and nonleptonic couplings and form factors, with some notable exceptions; *e.g.*, the neutron's charge radius and axial vector coupling. Properly incorporating the lower component of the nucleon's spinor helps somewhat in addressing these exceptions. However, discrepancies

remain and I anticipate that their amelioration requires the inclusion of axial-vector diquark correlations and a pion cloud. With these features included, I will be able to calculate observables such as the  $N \rightarrow \Delta$  transition form factor, in which the resonant quadrupole strength can be interpreted as a signal of nucleon deformation.



### a.12. Valence-Quark Distributions in the Nucleon (C. D. Roberts)

The pion provides the simplest theoretical subject for a calculation of the valence quark distribution function. However, pion targets are not readily available for experiment and the most reliable measurements of quark distribution functions have been performed on nucleon targets. I intend to extend the approach developed for the pion so as to employ it in a calculation of the nucleon's valence quark distribution. In the first studies, the target nucleon will be represented by a quark-plus-scalar-diquark product Ansatz for its Faddeev amplitude. This promises to provide the first Poincaré covariant calculation of the

nucleon's valence quark distribution function. Improving the nucleon model via the inclusion of axial-vector diquark correlations and a pion cloud will enable the drawing of a connection between deep inelastic scattering measurements and the "soft physics" wrapped up in nucleon structure. For example, it will provide a means of testing the validity and importance of diquark clustering in the nucleon, and the relation between the d/u-ratio at large-x and confinement, as it is exhibited in the momentum-space extent of the Faddeev amplitude.

### a.13 J/ψ Suppression as a Signal of Quark Gluon Plasma Formation (C. D. Roberts, D. B. Blaschke,\* and Yu. L. Kalinovsky†)

We have developed a successful approach to describing heavy-meson observables at zero temperature. That enables a reliable extrapolation into the domain of nonzero temperature, which is relevant to the RHIC program. The suppression of the J/ψ production cross section is touted as a unique signal of quark gluon plasma formation, and such a suppression has been observed at CERN. We propose to study J/ψ production in the expectation that additional insight will follow from the Dyson-Schwinger equations' capacity to unify nonperturbative aspects of light- and heavy-meson observables via a microscopic description using QCD's elementary excitations. Our initial focus is the

T-dependence of J/ψ break-up by hadronic comovers; i.e., the substructure induced T-dependence of those interactions with other mesons in the medium that dissociates the J/ψ. These processes are likely to be affected by the dramatic T-dependence of the dressed-light-quark mass function in the neighborhood of the QGP phase boundary and a possible T-dependent reduction in the mass of the open-charm final states. Our goal is to elucidate the mechanisms involved and the fidelity of J/ψ suppression as a signal of quark gluon plasma formation.

\*University of Rostock, Germany, †LCTA, JINR, Dubna, Russia

### a.14. Schwinger-Dyson Approach to Nonequilibrium Classical Field Theory (B. Mihaila, F. Cooper\*, J. Dawson†)

We discuss a Schwinger-Dyson [SD] approach<sup>1</sup> for determining the time evolution of the unequal time correlation functions of a non-equilibrium classical field theory, where the classical system is described by an initial density matrix at time  $t = 0$ . We focus on  $\lambda\phi^4$  field theory in 1+1 space-time dimensions where we can perform exact numerical simulations by sampling an ensemble of initial conditions specified by the initial density matrix. We discuss two approaches. The first, the bare vertex approximation [BVA], is based on ignoring vertex corrections to the SD equations in the auxiliary field formalism relevant for  $1/N$  expansions. The second approximation is a related approximation made to the SD equations of the original formulation in

terms of  $\phi$  alone. We compare these SD approximations as well as a Hartree approximation with exact numerical simulations. We find that both approximations based on the SD equations yield good agreement with exact numerical simulations and cure the late time oscillation problem of the Hartree approximation. We also discuss the relationship between the quantum and classical SD equations.

Our results give us confidence that this approximation will be useful in future studies of quantum phase transitions in the O(4) model. The fact that in homogeneous situations this approximation leads to thermalization will allow us to study the rate of

equilibration versus expansion rate for an expanding plasma undergoing a phase transition. We will then be able to see whether some of the interesting phenomena

occurring during the early stages of a chiral phase transition will survive the hard scatterings present in the BVA approximation.

---

\*Los Alamos National Laboratory, †University of New Hampshire

<sup>1</sup>B. Mihaila, F. Cooper, and J. Dawson, Phys. Rev. D **64**, 125003 (2001)

### a.15. Numerical Approximations using Chebyshev Polynomial Expansions (B. Mihaila and I. Mihaila\*)

We present numerical solutions<sup>1</sup> for differential equations by expanding the unknown function in terms of Chebyshev polynomials and solving a system of linear equations directly for the values of the function at the extrema (or zeros) of the Chebyshev polynomial of order  $N$  (El-gendi's method). The solutions are exact at these points, apart from round-off computer errors and

the convergence of other numerical methods used in connection with solving the linear system of equations. Applications to initial value problems in time-dependent quantum field theory and second order boundary value problems in fluid dynamics are presented.

---

\*Coastal Carolina University

<sup>1</sup>B. Mihaila and I. Mihaila, J. Phys. A: Math. Gen. **35**, 731 (2002)

### a.16. Dynamical Study of the $\Delta$ Excitation in $N(e,e'\pi)$ Reactions (T.-S. H. Lee and T. Sato\*)

We have completed our investigation of the  $\Delta$  excitation in pion electroproduction on the nucleon. It is found that the model can describe, to a very large extent, the recent data on  $p(e,e'\pi^0)$  and  $p(e,e'\pi^+)$  reactions from Jefferson Lab, as shown in Fig. V-3. The magnetic dipole (M1), electric dipole (E2), and Coulomb (C2) strengths of the  $\gamma N \rightarrow \Delta$  transition have been extracted. It is found that the C2/M1 ratio drops significantly with  $Q^2$  and reaches about -14% at  $Q^2 = 4$

(GeV/c)<sup>2</sup>, while the E2/M1 ratio remains close to the value  $\sim -3\%$  at the  $Q^2 = 0$  photon point. The extracted M1 transition form factor drops faster than the usual dipole form factor of the proton. We also find that the nonresonant interactions can dress the  $\gamma N \rightarrow \Delta$  vertex to significantly enhance its strength at low  $Q^2$ , but much less at high  $Q^2$ , as shown in Fig. V-4, for the Coulomb C2 form factor. A paper describing our results has been published.<sup>1</sup>

---

\*Osaka University, Japan

<sup>1</sup>T. Sato and T.-S. H. Lee, Phys. Rev. C **63**, 055201 (2001)

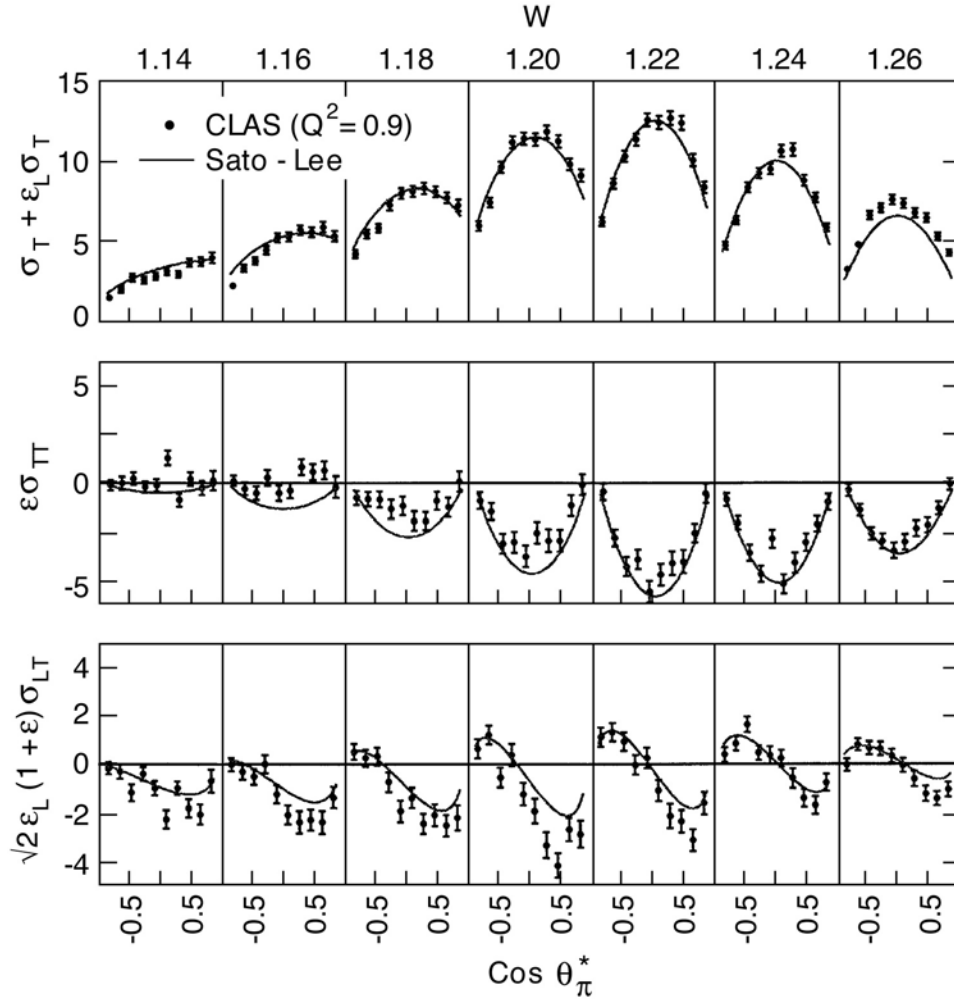


Fig. V-3. The predicted differential cross sections of  $p(e, e' \pi^0)$  reaction at  $Q^2 = 0.9 \text{ (GeV/c)}^2$  are compared with the 2001 data from Jefferson Lab.

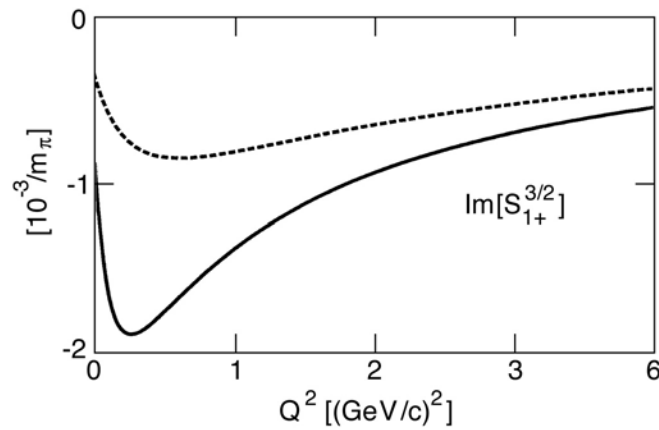


Fig. V-4. The predicted Coulomb  $C_2$  form factor of  $\gamma N \rightarrow \Delta$  is  $\propto \text{Im}[S_{1+}^{3/2}]$ . The dashed curve is obtained when the pion cloud effects are neglected.

### a.17. Nucleon Resonances in $\omega$ Photoproduction (T.-S. H. Lee, Yongseok Oh,<sup>\*</sup> and Alexander I. Titov<sup>†</sup>)

We have investigated the role of the nucleon resonances ( $N^*$ ) in  $\omega$  photo-production. In contrast with the previous investigations based on the  $SU(6) \times O(3)$  limit of the constituent quark model, the employed  $N^* \rightarrow \gamma N$  and  $N^* \rightarrow \omega N$  amplitudes include the configuration mixing effects due to the residual quark-quark interactions. The contributions from the nucleon resonances are found to be significant relative to the nonresonant amplitudes in changing the differential cross sections at large scattering angles. We suggest that a crucial test of our predictions can be made by measuring the parity asymmetry and beam-target double asymmetry at forward scattering angles. The

dominant contributions are found to be from  $N1/2^+(1910)$ , a missing resonance, and  $N3/2^-(1960)$  which is identified as the  $D_{13}(2080)$  of the Particle Data Group. A paper describing our results has been published.<sup>1</sup> We have extended our investigation to address the questions concerning the sub-threshold  $N^*$  excitation and the coupled-channel effects due to  $\pi N$  and  $\rho N$  channels. Both effects are found to be important and must be included in examining the  $N^*$  effects in energies near production threshold. Our results are shown in Fig. V-5. Two papers on this work are being prepared for publication.

<sup>\*</sup>Academia Sinica, Taiwan, <sup>†</sup>JINR, Dubna, Russia

<sup>1</sup>Y. Oh, A. I. Titov, and T.-S. H. Lee, Phys. Rev. C **63**, 025201 (2001)

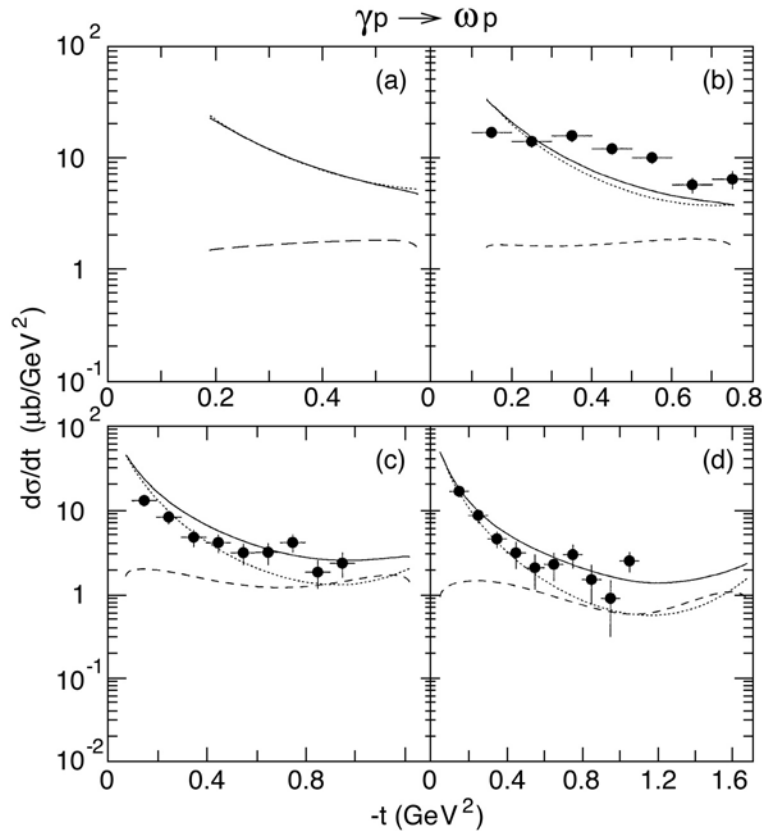


Fig. V-5. Coupled-channel effects on  $\omega$  photoproduction. The dotted curves are from the tree-diagram, and the dashed curves are from the effects due to the intermediate  $\pi N$  channel. The solid curves are from the coherent sum of these two mechanisms. The energies for the incoming photon are 1.16 (upper-left), 1.23 (upper-right), 1.45 (lower-left), and 1.68 (lower-right) GeV.

### a.18. The Pion Contributions to the $\gamma N \rightarrow \Delta$ Transition (T.-S. H. Lee, T. Nakamura,\* and T. Sato\*)

The  $\gamma N \rightarrow \Delta$  parameters extracted from the dynamical model developed in [Phys. Rev. C **54**, 2660 (1996), Phys. Rev. C **63**, 055201 (2001)] are analyzed within the chiral constituent quark model. By using the unitary transformation to separate the baryon bound state properties from the scattering dynamics, we show how the extracted bare  $\gamma N \rightarrow \Delta$  parameters can be related to the contributions from constituent quarks and virtual pion loops. It is found that the one-loop pion

contributions account for about 10% of the bare magnetic dipole (M1) transition. For the bare electric quadrupole (E2) and Coulomb (C2) strengths, the one-loop contributions are found to be in opposite sign of the values extracted from the data. This suggests that either the constituent quark configurations in  $\Delta$  and/or N have d-state components, or there exists non-pionic exchange-current contributions. A paper describing our results is being prepared for publication.

\*Osaka University, Japan

### a.19. Coupled-Channel Approach for $K^+\Lambda$ Photoproduction (T.-S. H. Lee, Wen-Tai Chiang,\* F. Tabakin,\* and B. Saghai†)

Kaon photoproduction on the nucleon is studied using a coupled-channel (CC) approach. A general method to include multi-step final-state interactions of electromagnetic strangeness production is developed, and then applied numerically to investigate the  $\gamma p \rightarrow K^+\Lambda$  process. In addition to direct  $K^+\Lambda$  production, we incorporate both  $\pi^0 p$  and  $\pi^+ n$  pion-nucleon channels in our CC approach. Cross sections are calculated and compared to recent data from SAPHIR, with emphasis

on the CC effects. We show that the CC effects due to the  $\pi N$  channels are significant at the level of inducing 20% changes in total cross sections; thereby demonstrating the need to include  $\pi N$  coupled-channels to correctly describe electromagnetic strangeness production. Our results on total cross sections are shown in Fig. V-6. A paper describing our results has been published.<sup>1</sup>

\*University of Pittsburgh, †CEA-Saclay, France

<sup>1</sup>W.-T. Chiang, F. Tabakin, T.-S. H. Lee, and B. Saghai, Phys. Lett. B **514**, 101 (2001)

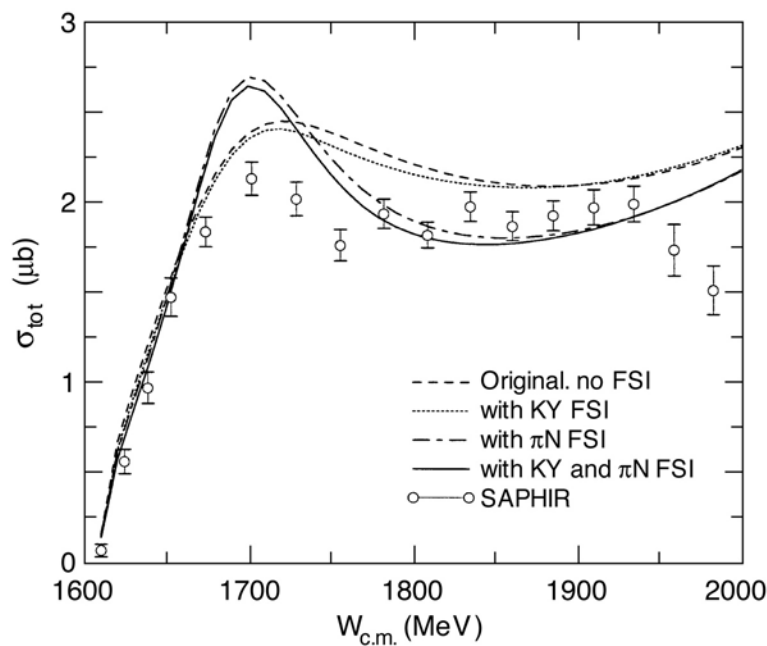


Fig. V-6. Coupled-channel effects of  $\gamma p \rightarrow K^+\Lambda$  reaction.

### a.20. Meson-Exchange $\pi$ N Models in Three-dimensional Bethe-Salpeter Formulation (T.-S. H. Lee, Cheng-Tsung Hung,\* and Shin Nan Yang†)

We have investigated pion-nucleon scattering by using several three-dimensional reduction schemes to the Bethe-Salpeter equation for a model Lagrangian involving  $\pi$ , N,  $\Delta$ ,  $\rho$ , and  $\sigma$  fields. It is found that all of the resulting meson-exchange models give similar good descriptions of the  $\pi$ N scattering data up to 400 MeV. However, they have significant differences in describing the  $\pi$ NN and  $\pi$ N $\Delta$  form factors and the  $\pi$ N

off-shell t-matrix elements. We show that these differences can best be distinguished by investigating the near-threshold pion production from nucleon-nucleon collisions and pion photoproduction on the nucleon. The consequences of using these models to investigate various pion-nucleus reactions are also discussed. A paper describing our results has been published.<sup>1</sup>

\*Chung-Hua Institute of Technology, Taiwan, †National Taiwan University

<sup>1</sup>C.-T. Hung, S. N. Yang, and T.-S. H. Lee, Phys. Rev. C **64**, 034309 (2001)

### a.21. $\phi$ -N Bound State (T.-S. H. Lee, H. Gao,\* and V. Marinov\*)

It has been suggested that the QCD van der Waals' interaction, mediated by multi-gluon exchange, is dominant when the interacting two-color singlet hadrons have no common quarks. We have found that such a QCD van der Waals' force is strong enough to bind a  $\phi$  meson onto a nucleon inside a nucleus to form

a bound state. The direct experimental signature for such an exotic state is proposed in the case of sub-threshold  $\phi$  meson photoproduction from a nuclear target. The predicted rates indicate the feasibility of such an experiment at JLab. A paper describing our results has been published.<sup>1</sup>

\*MIT

<sup>1</sup>H. Gao, T.-S. H. Lee, and V. Marinov, Phys. Rev. C **63**, 022201 (2001)

### a.22. Compressed Nuclei with $\Delta$ s and Hyperons (T.-S. H. Lee, Mahmoud A. Hasan,\* and James P. Vary†)

To interpret the data from relativistic heavy-ion collisions, we are continuing our effort to investigate compressed nuclei with  $\Delta$ 's and hyperons. The ground state properties of  $^{90}\text{Zr}$ ,  $^{100}\text{Sn}$ , and  $^{132}\text{Sn}$  at equilibrium and at large amplitude-compression have been investigated within the framework of the constrained spherical Hartree-Fock (CSHF) approximation. We use a realistic effective baryon-baryon Hamiltonian that includes the N-N, the N- $\Delta$ , and the  $\Delta$ - $\Delta$  interactions. We specifically investigate the sensitivity to the sizes of the nucleon and  $\Delta$  model spaces. At equilibrium, we find no case of mixing between nucleons and  $\Delta$ 's in our largest model space of eight major nucleon shells plus sixteen  $\Delta$  orbitals. On the contrary, there is mixing in  $^{90}\text{Zr}$  and  $^{132}\text{Sn}$  in the smaller model space of seven major nucleon shells plus eight  $\Delta$  orbitals. Expanding the nucleon model space has a larger effect on reducing the static compression modulus and softening the nuclear equation-of-state than increasing the number of  $\Delta$  states. Most of the excitation energy delivered to the

system during compression is employed by the two nuclei with a neutron excess (*i.e.*,  $^{90}\text{Zr}$ ,  $^{132}\text{Sn}$ ) to create the massive  $\Delta$  resonances. On the other hand, in the  $^{100}\text{Sn}$  nucleus most of the excitation energy goes to a simple reduction in the binding, suggesting a suppressed role for the  $\Delta$  states. Under extreme compression at a density 2-3 times normal nuclear density, the excitation of nucleons to  $\Delta$ 's increases sharply up to 10% of the total number of constituents. At finite excitation energy under compression, the number of  $\Delta$  excitations is not dependent on the number of  $\Delta$ -states over the range studied. The  $\Delta$ -excitation results are consistent with heavy-ion collision data, and suggest an important mean-field mechanism for sub-threshold pion production in particle-nucleus and nucleus-nucleus collisions. A paper describing our results has been published.<sup>1</sup> We are currently extending the approach to include hyperons in the calculation of compressed nuclei.

\*Applied Science University, Jordan, †Iowa State University, Ames

<sup>1</sup>Mahmoud A. Hasan, J. P. Vary, and T.-S. H. Lee, Phys. Rev. C **64**, 024306 (2001)

### a.23. Dynamical Study of the ${}^2\text{H}(e,e'\pi^+)$ Reaction (T.-S. H. Lee and K. Hafidi)

The  ${}^2\text{H}(e,e'\pi^+)$  reaction in parallel kinematics has been investigated using a dynamical model of pion electroproduction on the nucleon. A unitary  $\pi\text{NN}$  model has been used in order to examine the effects due to the final two-nucleon interactions, pion rescattering from the second nucleon, and intermediate  $\text{NN}$  and  $\text{N}\Delta$  interactions. Our results are compared with the data in Fig. V-7. It has been found that these  $\pi\text{NN}$  mechanisms are small, but they can have significant contributions to the  ${}^2\text{H}(e,e'\pi^+)$  cross sections through

their interference with the dominant impulse term. For the longitudinal cross sections, the effects due to the interference between the pion pole term and other production mechanisms are also found to be very large. Our findings clearly indicate that these interference effects must be accounted for in any attempt to determine from the  ${}^2\text{H}(e,e'\pi^+)$  data whether the pion form factor and/or  $\pi\text{NN}$  vertex of the pion pole term are modified in the nuclear medium. This work has been published.<sup>1</sup>

<sup>1</sup>K. Hafidi and T.-S. H. Lee, Phys. Rev. C **64**, 064607 (2001)

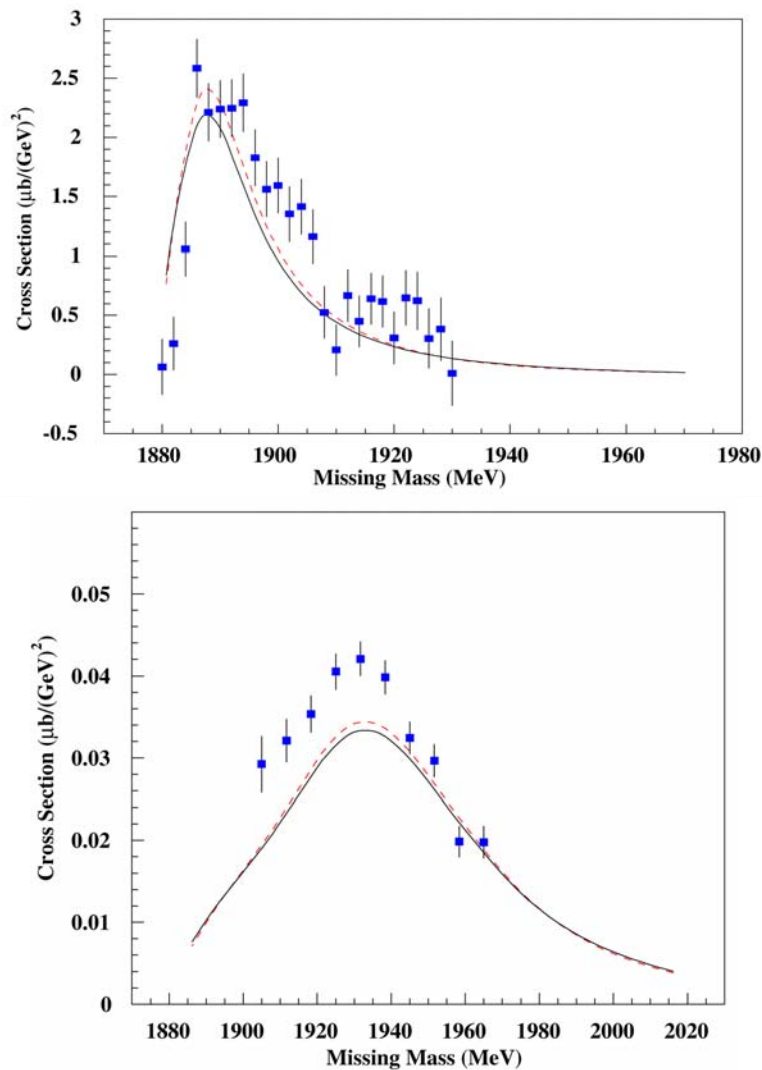


Fig. V-7. The calculated  ${}^2\text{H}(e,e'\pi^+)$  cross sections in the parallel kinematics are compared with the data from Saclay, 1992 (top), and Jefferson Laboratory, 2001 (bottom). The dashed curves are obtained from neglecting the final  $\text{NN}$  interactions.

### a.24. $\eta$ Meson Production in NN Collisions (T.-S. H. Lee, K. Nakayama,\* and J. Speth†)

$\eta$  meson production in both proton-proton and proton-neutron collisions is investigated within a relativistic meson exchange model of hadronic interactions. It is found that the available cross section data can be described equally well by either the vector or pseudoscalar meson exchange mechanism for exciting

the  $S_{11}(1535)$  resonance. Our results are compared with the data in Fig. V-8. It is shown that the analyzing power data can potentially be very useful in distinguishing these two scenarios for the excitation of the  $S_{11}(1535)$  resonance. A paper describing our results has been submitted for publication.

\*University of Georgia, †Forschungszentrum-Jülich, Germany

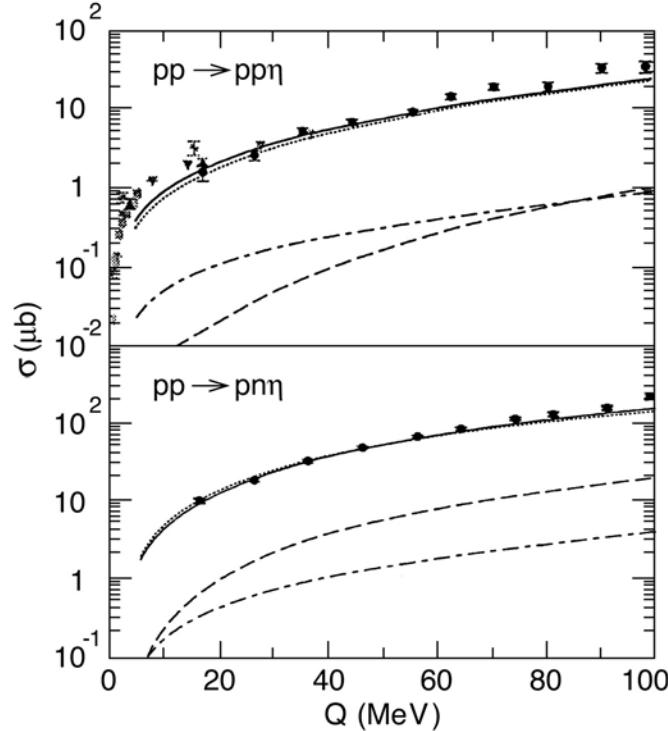


Fig. V-8 Total cross sections for  $pp \rightarrow pp\eta$  (upper panel) and  $pn \rightarrow pn\eta$  (lower panel). The dashed curves correspond to nucleonic current contribution while dot-dashed curves correspond to mesonic current contribution; the dotted curves represent the resonance current contribution. The solid curves are the total contributions.

### a.25. Study of Nucleon Resonances with Double Polarization Observables in Pion Photoproduction (T.-S. H. Lee, D. Dutta,\* and H. Gao\*)

Motivated by new experimental opportunities at Jefferson Lab, the role of nucleon resonances in the double polarization observables of pion photoproduction is investigated. As an example, we show that the not-well-determined two-star resonance

$N_{3/2}(1660)$  can be examined by performing experiments on beam-recoil polarization at large angles. A paper describing our results has been submitted for publication.

\*MIT



**a.26. From Light Nuclei to Nuclear Matter: The Role of Relativity** (F. Coester)

The success of non-relativistic quantum dynamics in accounting for the binding energies and spectra of light nuclei<sup>1</sup> with masses up to  $A = 10$  raises the question whether the same dynamics, applied to infinite nuclear matter, agrees with the empirical saturation properties of large nuclei. Nuclear matter results of comparable accuracy for realistic Hamiltonians should become available. The simple unambiguous relation between few-nucleon and many-nucleon Hamiltonians is directly related to the Galilean covariance of nonrelativistic dynamics. Relations between the irreducible unitary representations of the Galilei and Poincaré groups indicate that the “nonrelativistic” nuclear Hamiltonians may provide sufficiently accurate approximations to Poincaré invariant mass operators.

There is, however, no firm theoretical basis for a prediction that there are “realistic” Hamiltonians which fit the empirical nuclear matter properties without additional many-body forces.

The essential feature of “relativistic” nuclear dynamics<sup>2</sup> is that the intrinsic nucleon parity is an explicit, dynamically relevant degree of freedom. The success of this approach to nuclear matter and large nuclei suggests the question how it might account for the spectral properties of light nuclei. Can hypothetical “realistic” Hamiltonians acting on tensor products of spinor functions account for both light nuclei and nuclear matter without a need for many-body forces?

<sup>1</sup>Steven C. Pieper and R. B. Wiringa, *Ann. Rev. Nucl. Sci.* **51**, 53 (2001)

<sup>2</sup>Brian D. Serot and John Dirk Walecka, *Int. J. of Mod. Phys.* **E6**, 515 (1997)

**a.27. Null-Plane Dynamics of Elastic Electron Deuteron Scattering** (F. Coester and W. N. Polyzou\*)

It is an inescapable feature of relativistic Hamiltonian dynamics that single-particle current density operators are covariant only under the kinematic subgroup. Null-plane dynamics has the unique feature that, like Galilei covariant dynamics, it allows a consistent impulse approximation, provided the momentum transfer is in the null plane. Model-independent interaction currents are introduced by the requirements of rotational covariance. They depend on the angle between the null vector and the transverse polarization vector used in the

computation of form factors. We find that the null-plane impulse approximation, with the null vector in the direction of the transverse canonical polarization vector together with a recent parameterization of the nucleon form factors,<sup>1</sup> provides a good representation of the deuteron structure functions A and B as shown in Fig. V-9. Covariant meson-exchange currents<sup>2</sup> can be added consistently in this framework. A quantitative investigation of meson-exchange currents is in progress.

\*University of Iowa

<sup>1</sup>E. L. Lomon, *Phys. Rev. C* **64** 035204 (2001)

<sup>2</sup>F. Coester and D. O. Riska, *Ann. Phys.* **234**, 141 (1994)

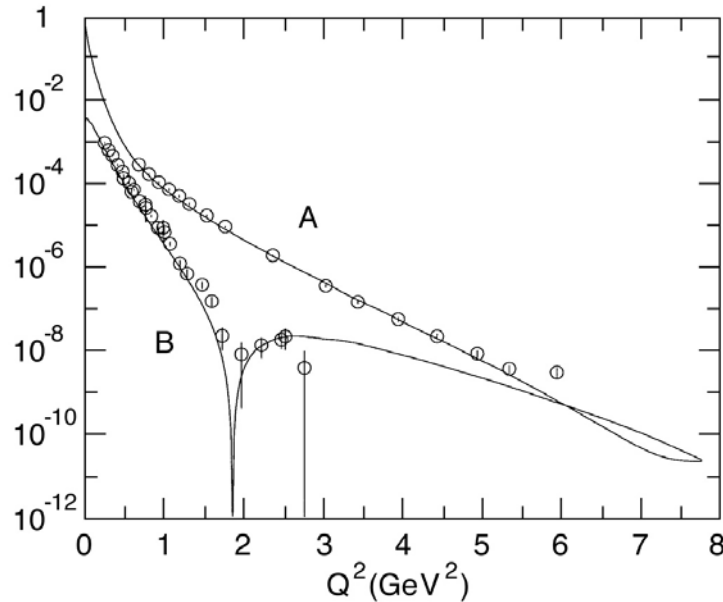


Fig. V-9. Null-plane impulse approximation of the deuteron structure functions A and B.

## B. NUCLEAR FORCES AND NUCLEAR SYSTEMS

The goal of this program is to achieve a description of nuclear systems ranging in size from the deuteron and triton to nuclear matter and neutron stars using a single parameterization of the nuclear forces. Aspects of our program include both the construction of two- and three-nucleon potentials and the development of many-body techniques for computing nuclear properties with these interactions. Detailed quantitative, computationally-intensive studies are essential parts of this program.

Quantum Monte Carlo (QMC) calculations of light ( $A \leq 10$ ) nuclei with realistic interactions have been the main focus of our recent efforts. Our nonrelativistic Hamiltonian contains the accurate Argonne  $v_{18}$  two-nucleon (NN) potential, which includes charge-independence breaking terms, and either the venerable Urbana IX three-nucleon (NNN) potential, or one of several new Illinois NNN models. The QMC calculations include both variational (VMC) and Green's function (GFMC) methods. We begin with the construction of variational trial functions based on sums of single-particle determinants with the correct total quantum numbers, and then act on them with products of two- and three-body correlation operators. Energy expectation values are evaluated with Metropolis Monte Carlo integration and parameters in the trial functions are varied to minimize the energy. These optimized variational wave functions can then be used to study other nuclear properties. They also serve as a starting point for the GFMC calculations, which systematically remove higher excited-state components from the trial wave functions by a propagation in imaginary time.

We are currently studying all  $A \leq 10$  nuclei with experimentally known bound state or resonance energies, including some 55(30) excited states in VMC (GFMC). These are the first calculations treating  $A \geq 6$  nuclei directly with realistic NN and NNN interactions. In GFMC calculations,

with the new Illinois NNN models, we can reproduce most of the experimental ground- and excited-state energies within 0.5 MeV. The VMC calculations, including two-body charge and current operators, are being used to study weak decays of  $A = 6-8$  nuclei and for various  $(e,e'p)$  and  $(e,e'n)$  reactions. They are also being used to obtain astrophysically interesting cross sections, such as  ${}^2\text{H}(\alpha,\gamma){}^6\text{Li}$  and  ${}^3\text{He}(\alpha,\gamma){}^7\text{Be}$ . Finally, we are also studying the properties of neutron drops with the goal of providing additional constraints for the construction of Skyrme interactions that are used in the modeling of neutron-rich nuclei in neutron star crusts.

In addition, a new effort using the coupled cluster  $[\text{exp}(S)]$  method was initiated last year. The coupled cluster method is being used to study nuclei in the  ${}^{12}\text{C}$ - ${}^{16}\text{O}$  range, using the same realistic Hamiltonian as the quantum Monte Carlo calculations. Comparisons of GFMC and  $\text{exp}(S)$  results are being made for  ${}^4\text{He}$  and neutron drops. We are also able to compare both methods with results of traditional shell model calculations. Finally, studies of hypernuclei are also continuing, particularly the charge-symmetry-breaking of  $\Lambda\text{N}$  interactions.

### **b.1. Quantum Monte Carlo Calculations of Light p-shell Nuclei** (S. C. Pieper, R. B. Wiringa, J. Carlson,\* V. R. Pandharipande,† and K. Varga‡)

Since the early 1990s, we have been studying the ground and low-lying excited states of light p-shell nuclei as  $A$ -body problems with realistic nucleon-nucleon (NN) and three-nucleon (NNN) interactions using advanced quantum Monte Carlo (QMC) methods. Our preferred Hamiltonians contain the Argonne  $v_{18}$  NN potential, which gives an excellent fit to elastic NN scattering data and the deuteron energy and Illinois NNN potentials, which were fit to binding energies of  $A \leq 8$  nuclei, as described in the next section. The QMC methods include both variational Monte Carlo (VMC), which gives an initial approximate solution to the many-body Schrödinger equation, and the Green's function Monte Carlo (GFMC), which systematically improves on the VMC starting point and produces binding energies that are accurate to within 2%. This year we have concentrated on  $A = 9, 10$  nuclei, and have made our first variational unnatural-parity-state calculations.

The VMC calculations begin with the construction of an antisymmetric Jastrow trial wave function that includes single-particle orbits coupled to the desired JM values of the state of interest as well as pair and triplet spatial correlations. It is then acted on by a symmetrized product of two-body spin, isospin, tensor, and spin-orbit correlation operators, induced by the NN potential, and three-body correlation operators for the NNN potential. The wave functions are diagonalized in the small basis of different Jastrow spatial symmetry components to project out higher excited states with the same quantum numbers.

In the GFMC calculations, we operate on a version of the VMC trial function with the imaginary time propagator,  $\exp[-(H'-E_0)\tau]$ , where  $H'$  is a simplified Hamiltonian,  $E_0$  is an estimate of the eigenvalue, and  $\tau$  is the imaginary time. The excited-state components of the trial function will then be damped out for large  $\tau$ , leaving the exact lowest eigenfunction with the quantum numbers of the input variational wave function. The expectation value of  $H$  is computed for a sequence of increasing values of  $\tau$  to determine the convergence. Our  $H'$  contains the reprojected  $v_8$  part of the NN potential and the full NNN potential. The small correction,  $H-H'$ , is computed perturbatively. The many-body propagator is written as a symmetrized product of exact two-body propagators, with the NNN potential treated in lowest order.

In previous years we have made significant improvements in the GFMC algorithms, especially in solving the fermion sign problem for nuclear systems. The method and program now seems stable and we have concentrated on extending the calculations to larger nuclei and on developing new models of the NNN potential. The computer resources (both CPU time and memory) required for these calculations increase exponentially with the number of nucleons. Therefore, progress to bigger nuclei usually requires a new generation of computers.

Phase-II of the IBM SP at NERSC was installed this year and we obtained a large amount of friendly-user time on it. As a demonstration of the scalability of our

GFMC program, we ran a more than 6-hour calculation of the  $1^-$  state of  $^{10}\text{Be}$  using 2048 processors. The sustained speed was 0.55 TFLOPS with a 92% speedup efficiency (that is the program ran 1886 times faster than it would have on just one processor). Due to scheduling considerations we routinely use only 256 to 512 processors. In addition to using the NERSC SP, we

continue to make extensive use of the Argonne Mathematics and Computer Science Linux cluster.

An Annual Reviews of Nuclear and Particle Science article describing our calculations of  $A \leq 8$  nuclei was published this year.<sup>1</sup>

\*Los Alamos National Laboratory, †University of Illinois, Urbana, ‡Oak Ridge National Laboratory

<sup>1</sup>S. C. Pieper and R. B. Wiringa, Ann. Rev. Nucl. Part. Sci. **51**, 53-90 (2001)

## b.2. Studies of Three-Nucleon Interactions in Nuclear Systems (S. C. Pieper, R. B. Wiringa, V. R. Pandharipande,\* D. G. Ravenhall,\* and J. Carlson†)

Our GFMC calculations of nuclei with  $3 \leq A \leq 8$  using the Hamiltonian consisting of the Argonne  $v_{18}$  two-nucleon (NN) and Urbana IX three-nucleon (NNN) potentials have shown that this Hamiltonian underbinds p-shell nuclei by 0.8 MeV in  $^6\text{Li}$  to 5 MeV in  $^8\text{He}$ . The error increases with both  $A$  and  $|N-Z|$ . This year we finished constructing improved “Illinois” models for the NNN potential.

softer cutoff parameter (normally we use the same cutoff as is used in the NN potential). Most of the models have the two-pion s-wave term with the strength preferred by chiral perturbation theory, but one of the models omits this term. In all, five Illinois models have been developed with various strengths for the four potential terms. All of them give excellent fits to the  $3 \leq A \leq 8$  binding energies – the rms errors are  $\leq 500$  keV. These results have been published.<sup>1</sup>

Our approach is to use theoretical guidance to suggest the structure of new terms, but to consider the coupling constants and short-range shapes of the potential to be adjustable. This is in the same spirit as the development of realistic NN potentials. We have considered a number of new terms. We find that new potential terms are often not perturbative, *i.e.*, an expectation value of the new term using the GFMC wave function from just Argonne  $v_{18}$  and Urbana IX may be misleading. Thus each new term must be added to the GFMC propagator and a new GFMC calculation made. Furthermore, as the strength of the new term is adjusted, the propagations must be repeated.

This year we have made an extensive set of  $A = 9, 10$  calculations with these new potentials. The reproduction of the nuclear levels continues to be satisfactory, although there is more dispersion than for  $A \leq 8$ . Preliminary calculations of nuclear matter with these potentials also show significant differences between the models. Figure V-10 compares GFMC values of ground and excited state energies for Argonne  $v_{18}$  with no NNN potential and one of the new Illinois models to experimental values. One sees the very important contributions made by the NNN potential to the p-shell binding energies, and the generally very good resulting agreement with the data.

The dominant term of the Urbana potential is the Fujita-Miyazawa (FM) two-pion term with intermediate excitation of one nucleon to a  $\Delta$ . We have now studied three-pion ring terms containing one and two  $\Delta$  excitations. These are repulsive in s-shell nuclei and attractive in p-shell nuclei and correct the overall loss of binding energy with respect to both  $A$  and  $|N-Z|$ . The Tucson-Melbourne potential contains the FM term and a two-pion term arising from s-wave  $\pi N$  scattering; we have also considered a corrected s-wave term.

A very interesting result can be seen in the  $^{10}\text{B}$  spectra. Experimentally the ground state of  $^{10}\text{B}$  is a  $3^+$  state. However the calculation with just AV18 very strongly predicts that the ground state is  $1^+$ . Petr Navratil (Livermore) first found this result using the no-core shell model and has shown that it is also true if the CD Bonn NN potential is used. Figure V-10 shows that including the Illinois-2 NNN potential results in the correct ground state. This is also true for the other Illinois potentials, but the older Urbana-IX potential also gives a  $1^+$  ground state.

The FM terms in the Urbana NNN potentials and the new models that we first constructed have coupling constants that are about  $\frac{1}{2}$  the value suggested by soft-pion physics. We have also made a model that has the stronger coupling constant; this required a significantly

\*University of Illinois, Urbana, †Los Alamos National Laboratory

<sup>1</sup>S. C. Pieper, V. R. Pandharipande, R. B. Wiringa, and J. Carlson, Phys. Rev. C **64**, 014001,1-21 (2001)

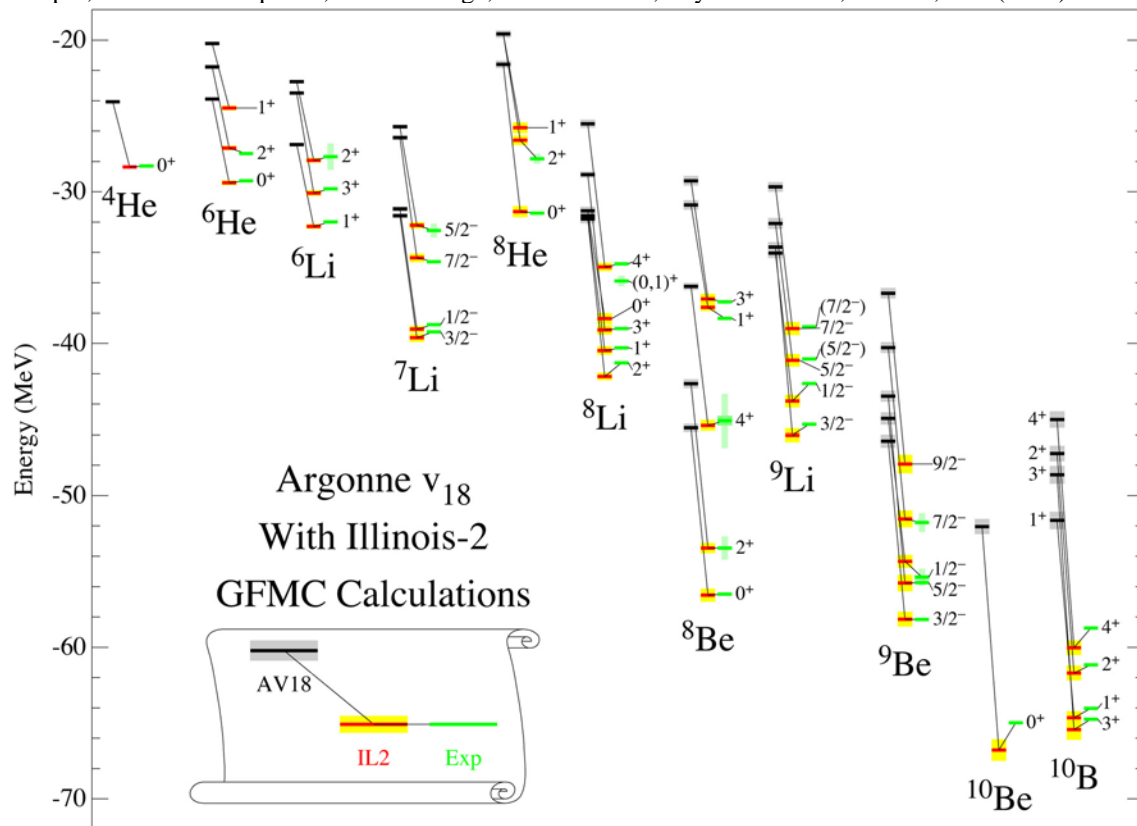


Fig. V-10. GFMC energies for  $A = 4-10$  nuclei using the Argonne  $v_{18}$  NN potential by itself and with one of the new Illinois NNN potentials, compared to experiment.

### b.3. What Makes Nuclear Level Structure? (S.C. Pieper and R.B. Wiringa)

As shown in the previous section, a Hamiltonian consisting of realistic, and hence complicated, NN and NNN potentials can accurately reproduce the level structure of light p-shell nuclei. We have investigated the effects of attempting to simplify the Hamiltonian. The previous section shows that the NNN potential is necessary to get the correct overall binding of all  $A \geq 3$  nuclei and further that something like the sophisticated new Illinois potentials seems necessary to get the correct  $3^+$  ground state of  $^{10}\text{B}$ .

In this study we made a series of calculations using no NNN potential and increasingly simpler versions of the Argonne  $v_{18}$ . In these NN potentials we kept a subset of the operators (for example AV8' contains central, spin-spin, tensor and spin-orbit terms with and without isospin exchange) and refit the radial forms to reproduce as many of the NN phase shifts as possible. Thus AV8' reproduces the  $^1\text{S}_0$ ,  $^3\text{S}_1$ - $^3\text{D}_1$ ,  $^1\text{P}_1$ , and  $^3\text{P}_{0,1,2}$  phase shifts. Next AV6' has no spin-orbit operators and

hence has very poor, almost degenerate,  $^3\text{P}_{0,1,2}$  phase shifts. The AV4' has no tensor operators and so no  $^3\text{S}_1$ - $^3\text{D}_1$  mixing; the deuteron still has the correct binding energy, but has no D-wave. The AV2' has no spin-spin operator and hence reproduces only the  $^1\text{S}_0$  and  $^3\text{S}_1$  phases; the P-wave phases are attractive. Finally AV1' is an average of the two terms in AV2' and binds the deuteron with only 0.43 MeV.

These potentials give increasingly poor representations of nuclear structure as is shown in Fig. V-11. The AV8' (not shown) is generally close to full results with some spin-orbit splittings being too small and the same inversion of levels in  $^{10}\text{B}$  as shown above. However the AV6' results in degenerate spin-orbit pairs. The AV4' does not mix different spatial symmetry states so the symmetry becomes a good quantum number. Also it results in too much binding as  $A$  increases. The AV2', with no repulsion in P waves, has lost all nuclear saturation; for example  $^5\text{He}$  is much more bound than

$^4\text{He}$ . Also, because of the repulsive core in the potential, the lowest spatial symmetry states become the ground states of the nuclei instead of the highest spatial symmetry states. With AV1' the overbinding with increasing A is even worse and, since the only thing distinguishing neutrons from protons is the Coulomb

potential, the valley of stability becomes severely distorted; the helium isotopes are the most bound A = 4 to 10 nuclei. Thus one really needs the full complication of the NN and NNN potentials to get a realistic picture of nuclear level structure.

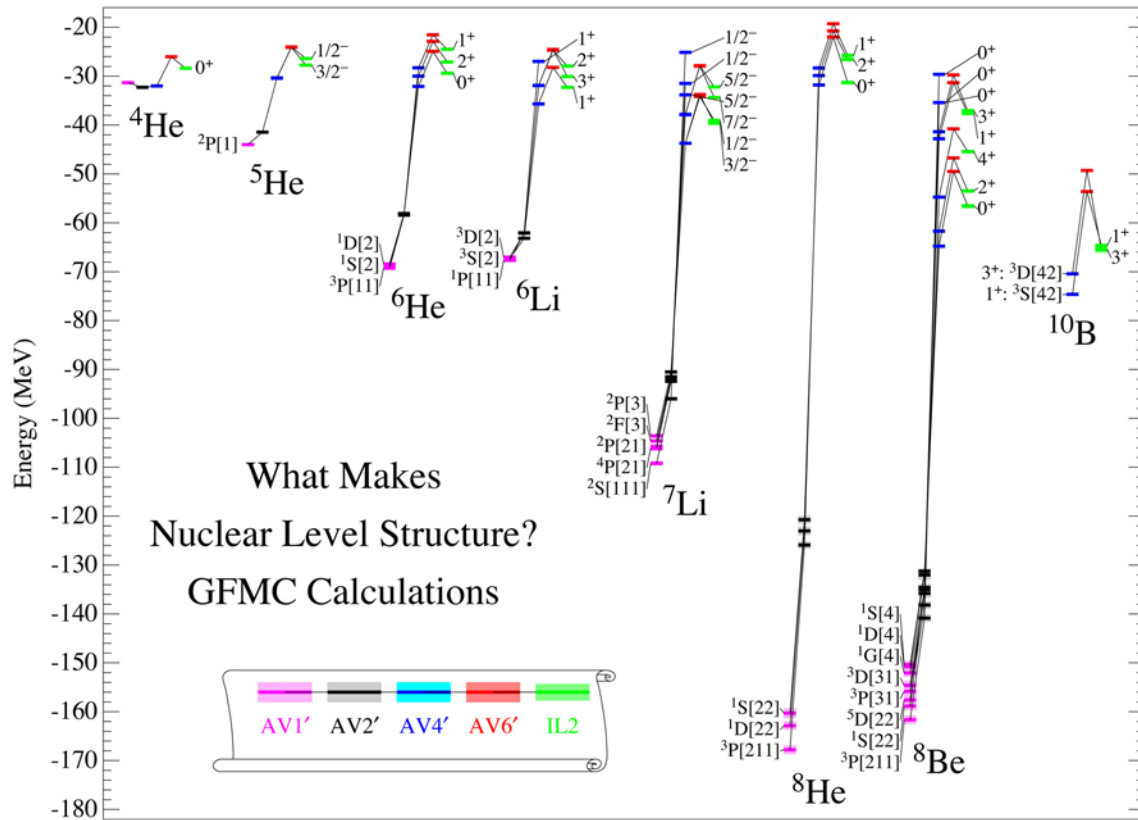


Fig. V-11. Energies of nuclear states using simplified Hamiltonians compared to results using a very complete Hamiltonian (AV18 + IL2).

**b.4. Radiative Capture Reactions for Astrophysical Applications** (R. B. Wiringa, K. M. Nollett,\* and R. Schiavilla†)

Radiative capture reactions play a major role in many astrophysical processes, including primordial nucleosynthesis and stellar evolution, yet they are frequently very difficult to measure accurately in the laboratory because of their small cross sections. We have used the many-body variational Monte Carlo (VMC) wave functions for the Argonne  $v_{18}$  two-nucleon and Urbana IX three-nucleon potentials discussed above to study three capture reactions involving light p-shell nuclei:  $^2\text{H}(\alpha,\gamma)^6\text{Li}$ ,  $^3\text{H}(\alpha,\gamma)^7\text{Li}$ , and  $^3\text{He}(\alpha,\gamma)^7\text{Be}$ . These reactions are responsible for the primordial lithium abundance, and the last one is also important in solar neutrino production.

We evaluated the appropriate matrix elements (primarily E1 and E2) between initial 4+2- or 4+3-body clusters, and the final 6- or 7-body ground state. The VMC wave functions were used for all clusters, supplemented by a suitable optical potential found in the literature for the initial cluster-cluster scattering state. The problem factorizes into a one-dimensional energy-dependent integral and a multi-dimensional energy-independent kernel. The latter is over the coordinates of all particles and requires significant computation; it is evaluated by standard Metropolis Monte Carlo techniques. The outer integral, over the cluster-cluster separation, is evaluated for a large

number of energies, and also with different choices for the folding optical potential, at little additional cost.

Results for the  ${}^2\text{H}(\alpha,\gamma){}^6\text{Li}$  reaction<sup>1</sup> were presented in last year's annual report; here we show in Fig.V-12 the final results for the  ${}^3\text{H}(\alpha,\gamma){}^7\text{Li}$  and  ${}^3\text{He}(\alpha,\gamma){}^7\text{Be}$  reactions, which served as the University of Chicago Ph.D. thesis work of Ken Nollett.<sup>2</sup> The  ${}^3\text{H}(\alpha,\gamma){}^7\text{Li}$  reaction was measured very accurately by Brune *et al.* in 1999, and for one choice of the optical potential our calculation agrees extremely well with the data. However, the measurements of the  ${}^3\text{He}(\alpha,\gamma){}^7\text{Be}$  reaction show a very large dispersion, and our calculations only touch the bottom edge of the data.

From our viewpoint, the data sets for the two reactions are not compatible.

The theoretical calculations can be improved in the future by: 1) using the more accurate GFMC wave functions, particularly for the p-shell final states; 2) using the better Illinois three-nucleon potentials discussed above, which give improved binding in the p-shell nuclei, to generate the cluster wave functions; and 3) using Monte Carlo techniques to develop consistent cluster-cluster scattering wave functions instead of depending on an external optical potential. It should also be possible to extend these calculations to additional reactions of astrophysical interest such as  ${}^7\text{Be}(p,\gamma){}^8\text{B}$ .

\*Present address: California Institute of Technology, †TJNAF and Old Dominion University

<sup>1</sup>K. M. Nollett, R. B. Wiringa, and R. Schiavilla, Phys. Rev. C **63**, 024003 (2001)

<sup>2</sup>K.M. Nollett, Phys. Rev. C **63**, 054002 (2001)

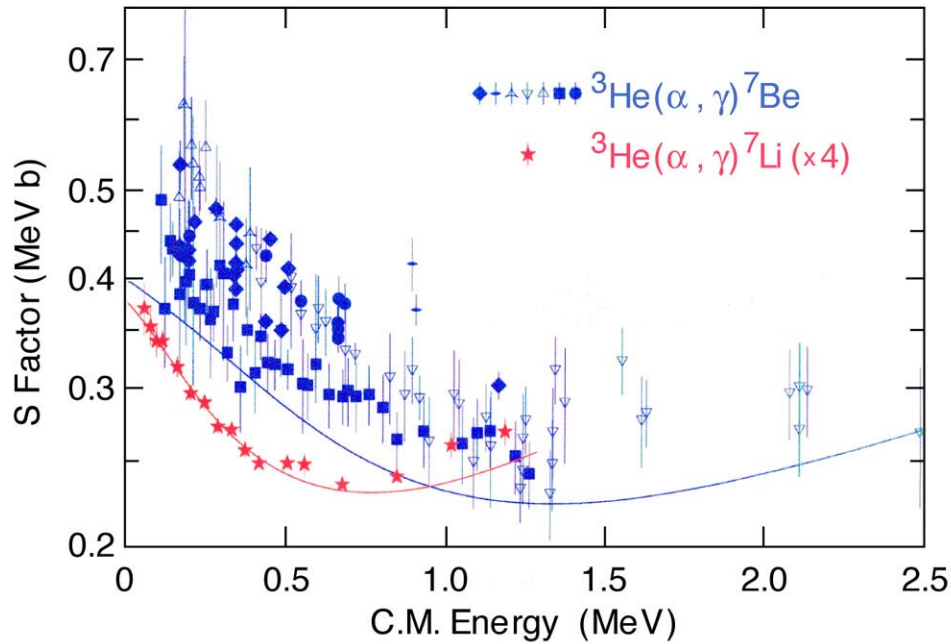


Fig. V-12. The total s-factor for  $\alpha+{}^3\text{H}$  and  $\alpha+{}^3\text{He}$  radiative capture compared to experimental data.

### b.5. Microscopic Calculations of A = 6-8 Weak Decays (R. B. Wiringa, S. C. Pieper, and R. Schiavilla\*)

We have studied the  ${}^6\text{He}$  beta decay and  ${}^7\text{Be}$  electron capture processes using variational Monte Carlo (VMC) wave functions, derived from a realistic Hamiltonian containing the Argonne  $v_{18}$  two-nucleon and Urbana IX three-nucleon interactions. The model for the nuclear weak axial current includes one- and two-body operators with the strength of the leading two-body term, associated with  $\Delta$ -isobar excitation of the nucleon, adjusted to reproduce the Gamow-Teller matrix element in tritium  $\beta$ -decay. The measured half-life of  ${}^6\text{He}$  is under-predicted by  $\cong 8\%$ , while that of  ${}^7\text{Be}$  for decay into the ground and first excited states of  ${}^7\text{Li}$  is over-predicted by  $\cong 9\%$ . However, the experimentally known branching ratio for these latter processes is in good agreement with the calculated value. Two-body axial current contributions lead to a  $\cong 1.7\%$  (4.4%) increase in the value of the Gamow-Teller matrix element of  ${}^6\text{He}$  ( ${}^7\text{Be}$ ), obtained with one-body currents only, and slightly worsen (appreciably improve) the agreement between the calculated and measured half-life. Corrections due to retardation effects associated with the finite lepton momentum transfers involved in the decays, as well as contributions of suppressed transitions induced by the

weak vector charge and axial current operators, have also been calculated and found to be negligible. A paper describing this work has been accepted for publication.<sup>1</sup>

Several improvements in these calculations are being prepared, including the use of the improved Illinois three-body potentials in the Hamiltonian, and the use of Green's function Monte Carlo wave functions instead of the VMC trial functions. We have also made initial VMC calculations of the more complicated A = 8 weak decays. While the A = 6 and 7 decays are between states of predominantly the same spatial symmetry, the decays of  ${}^8\text{He}$ ,  ${}^8\text{Li}$ , and  ${}^8\text{B}$  involve transitions where the spatial symmetry of the initial state is only a small component in the final state. An additional complication is that the  ${}^8\text{Li}$  and  ${}^8\text{B}$  ground states both decay to the wide  $2^+$  first excited state of  ${}^8\text{Be}$ , which at present we approximate as a bound state. Initial calculations in impulse approximation give less than half of the experimental Gamow-Teller matrix element, indicating these will be much tougher transitions to explain.

---

\*TJNAF

<sup>1</sup>R. Schiavilla and R. B. Wiringa, to be published in Phys. Rev. C

### b.6. Coupled Cluster Expansion Approach to Calculating Ground State Properties of Closed Shell Nuclei (B. Mihaila and J. Heisenberg\*)

We continue our project regarding the quest for a realistic description of the ground state of closed-shell nuclei in the p-shell ( ${}^{12}\text{C}$ ,  ${}^{16}\text{O}$ ). These calculations use the coupled cluster method [CCM] in configuration space, together with a realistic nuclear interaction and currents, which are purposely consistent with the work done by the GFMC collaboration. Just as the GFMC method, the CCM formalism is an exact approach to solving the many-body problem. In the past year we have put a lot of effort into obtaining a good description

for the ground-state of  ${}^4\text{He}$ . The difficulty of this task resides in the fact that higher order corrections in the CCM hierarchy are  $1/A$ -type corrections, which are clearly increasingly important in lighter nuclei. When completed, this project will provide an accurate description of nuclear structure properties in the CCM framework, for a mass domain between A = 4 and 16, and effectively open the possibility of treating nuclei as heavy as  ${}^{40}\text{Ca}$  on an equal footing.

---

\*University of New Hampshire



### b.7. Neutron-Proton Density Differences in Nuclei (A. R. Bodmer and Q. N. Usmani\*)

We have studied the neutron/proton distributions in nuclei in a local density approach. We show explicitly, as was originally pointed out by one of the authors (A.R.B.), that the density dependence of the symmetry-energy density  $F(\rho)$  drives the difference of distributions in the absence of coulomb and density-gradient contributions. In this limit we obtain an explicit solution  $\lambda_m$ , in terms of  $F(\rho)$ , for  $\lambda = (\rho_n - \rho_p)/\rho$ . For  $F \equiv 1$ :  $\lambda_m = \lambda_0 \equiv (N-Z)/A$  and the difference between the neutron and proton rms radii is  $\delta r = 0$ . Additional contributions  $\delta\lambda$  to  $\lambda_m$  are treated variationally. The gradient term makes only a small contribution to  $\delta\lambda$ , and  $\lambda$  is thus effectively determined only by the nuclear-matter quantity  $F(\rho)$ . The coulomb energy pushes  $\rho_p$  out relative to  $\rho_n$ , thus reducing  $\delta r$ . Decreasing the coulomb energy is equivalent to increasing  $u_\tau$  (the coefficient of the asymmetry term in

the semi-empirical mass formula);  $e = 0$  corresponds to  $u_\tau = \infty$  and gives the maximum  $\delta r$  for a given  $F(\rho)$ . Our numerical results are for  $^{208}\text{Pb}$ , see Fig. V-13. For a large range of  $F(\rho)$  we find that  $\delta r$  and  $u_{S\tau}/u_\tau$  ( $u_{S\tau}$  is the calculated coefficient of the surface-symmetry energy) are approximately universal functions of a normalization integral  $N$  involving  $F^{-1}(\rho)$ , in particular for  $\delta r \leq 0.5$  fm ( $N-1 \leq 1.5$ ) when the dependence on  $N-1$  is one-valued and approximately linear for small  $\delta r$  ( $\delta r \cong 0$  for  $N = 1$ ). Then  $N$  is effectively determined by  $\delta r$ . For such  $N$  there is also a strong correlation between  $\delta r$  and  $u_{S\tau}/u_\tau$ , allowing an approximate determination of the latter from  $\delta r$ . At larger  $N$ ,  $\delta r$  has a maximum; absolutely of  $\cong 0.75$  fm (for  $e = 0$ ) and of  $\cong 0.65$  fm for realistic  $u_\tau \cong 25 - 35$  MeV.

\*Universiti Putra Malaysia, Malaysia

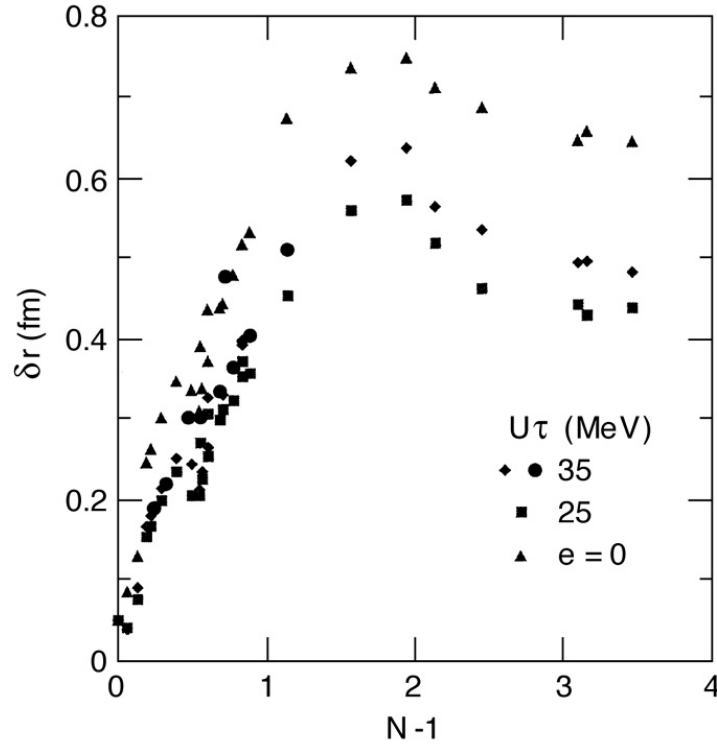


Fig. V-13. Difference  $\delta r$  between the neutron and proton rms radii.  $N$  is the norm of  $F_{(\rho\rho)}^{-1}$ , where  $F$  determines the density dependence of the symmetry-energy density.

### C. NUCLEAR STRUCTURE AND HEAVY-ION REACTIONS

This research focuses on nuclear structure in unusual regimes: nuclei far from stability, and superdeformed nuclei at high spin. We also study heavy-ion reactions near the Coulomb barrier. Much of this work is closely tied to experiments performed at ATLAS and at radioactive beam facilities.

Our studies of drip-line nuclei focus on breakup reactions, induced by the Coulomb and nuclear fields from a target nucleus. A critical issue is to develop a realistic description of the breakup mechanisms as a necessary tool for extracting nuclear structure properties of drip-line nuclei. We have applied our numerical technique of calculating the time-evolution of the two-body wave function for the relative motion of a halo nucleon and a core nucleus, in the time-dependent fields from a target nucleus, in order to test the validity of simpler reaction models, such as the eikonal approximation for the nuclear induced breakup, and first-order perturbation theory for Coulomb dissociation.

Our numerical studies of the nuclear induced breakup of  $^{11}\text{Be}$  on a light target show that the eikonal approximation becomes unrealistic at beam energies below 20 MeV/u. The breakup probabilities are reduced compared to the more realistic dynamical calculations. Our numerical studies of the Coulomb dissociation of  $^{17}\text{F}$  on high-Z targets show that first-order perturbation theory is also a poor approximation at lower energies. The leading order correction is a dynamical polarization effect of order  $Z^3$  in the target charge. We have also investigated other corrections, such as the Coulomb-nuclear interference and the effect of close collisions, where projectile and target have a non-zero overlap during the collision.

Our studies of the proton decay from nuclei beyond the proton drip-line are based on a coupled-channels technique. We have applied a particle-vibration model to analyze the decay from near-spherical proton emitters. The model explains very well the observed fine structure in the decay of  $^{145}\text{Tm}$ . Moreover, the spectroscopic factors predicted in a low-seniority shell model are reproduced much better when we include particle-vibration coupling.

Some nuclear structure problems of interest are superdeformation, heavy and superheavy elements, proton radioactivity, the neutron deficient Pb region and neutron-proton pairing near the  $N = Z$  line. To study these problems we make use of (1) the Strutinsky method as well as (2) self-consistent mean field (SCMF) calculations using the Gogny interaction, and (3) many-body (MB) wavefunctions.

In nuclides with roughly equal number of protons and neutrons,  $T = 1$  and  $T = 0$  n-p pairing will play an important role, in addition to the usual like-nucleon  $T=1$  pairing. To adequately treat and understand these effects, it is necessary to go beyond the quasiparticle approximation and to study not only those nuclei that are exactly on the  $N = Z$  line. The rare isotope accelerator (RIA) will provide considerable spectroscopic information on nuclides near the  $N = Z$  line. We have extended our many-body code to include neutron-proton pairing interactions. We have found that there is a new quantum number for characterizing collective states; *i.e.*, the number parity of the  $T = 0$  and  $T = 1$  n-p pairs.

Our studies of superdeformation at both low and high spins address the issue of possible new regions of superdeformation and hyperdeformation. Special emphasis is being put on the study of fission barriers at high spin as this is crucial for the possible production of very extended nuclei. We have studied nuclei with masses ranging from  $A \sim 80$  to  $A \sim 200$ , as a function of angular momentum, in a four-dimensional shape space using the Strutinsky method. We find several nuclides that are promising candidates for finding superdeformed and hyperdeformed shapes.

Our MB and SCMF calculations of nuclides in the neutron deficient Pb isotopes, in conjunction with J. L. Egido and L. M. Robledo, suggest the existence of many low-lying  $0^+$  excited states in this region. Experimental searches for these states are being carried out.

### c.1. Multipole Expansion for Relativistic Coulomb Excitation (H. Esbensen and C. A. Bertulani\*)

A theoretical description of relativistic Coulomb excitation has previously only been developed for distant collisions,<sup>1</sup> where projectile and target do not overlap. This description is often sufficient for reactions of stable nuclei but in reactions of proton-rich nuclei, where the density of the valence protons extends to large distances, one would also have to consider close collisions, where projectile and target penetrate each other. We have therefore studied<sup>2</sup> a general multipole expansion of the relativistic electromagnetic interaction between colliding nuclei, based on the Liénard-Wiechert potential and the associated current interaction. The Lorentz contraction introduces a deformation of this potential, and the multipole expansion will therefore contain diagonal as well as off-diagonal multipole components.

We have focused on monopole, dipole, and quadrupole single-particle excitations. For close collisions ( $r > r'$ , where  $r$  is the single-particle distance from the core, and  $r'$  is the projectile-target distance), the sum over off-diagonal components is finite but it is in principle infinite for distant collisions ( $r < r'$ ). We have made a simple truncation in the sum over the off-diagonal

components, including just the monopole and quadrupole terms associated with the deformation of the Liénard-Wiechard potential. We have tested this approximation in first-order perturbation theory for distant collisions (including the contributions from the current interaction) against the exact answer of Ref. [1]. We find that the approximation is quite accurate at least up to  $v/c = 0.6$ . This is illustrated in Fig. V-14, where the approximate longitudinal ( $m = 0$ ) and transverse ( $m = 1$ ) dipole excitation amplitudes are shown (in reduced units) by open symbols. The solid curves are the exact results,<sup>1</sup> whereas the dashed curves are the non-relativistic results. It is seen that the approximate results are essentially identical to the exact answer.

The multipole form factors we have derived can be used in higher-order dynamical calculations of the relativistic Coulomb dissociation of halo nuclei. Finite size effects can be implemented numerically in a straightforward manner. The truncated expansion discussed above should be reliable up to a few hundred MeV per nucleon, which is sufficient for experiments performed at most fragmentation facilities. This work has been published.<sup>2</sup>

\*Brookhaven National Laboratory

<sup>1</sup>A. Winther and K. Alder, Nucl. Phys. A319, 518 (1979)

<sup>2</sup>H. Esbensen and C. A. Bertulani, Phys. Rev. C 65, 024605 (2002)

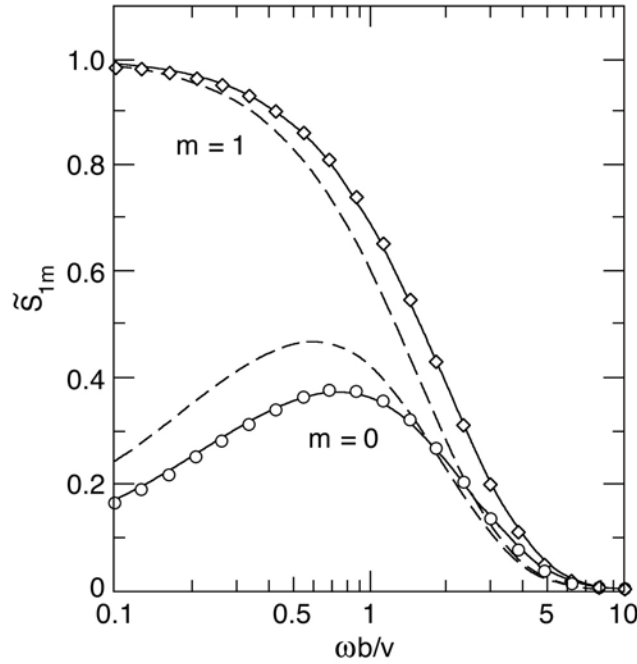


Fig. V-14. Excitation amplitudes (in reduced units) for longitudinal ( $m = 0$ ) and transverse ( $m = 1$ ) dipole excitations at distant collisions are shown as functions of the adiabaticity parameter  $\omega b/v$ , for  $v/c = 0.6$ . Approximate results (open symbols) are compared to exact results (solid curves) and to the non-relativistic results (dashed curves).

## c.2. Vibrational Interpretation of Spherical and Near-Spherical Proton Emitters

(C. N. Davids and H. Esbensen)

There has been a recent observation of fine structure in the proton decay of  $^{145}\text{Tm}$ .<sup>1</sup> The ground-state and fine structure groups have energies of 1.728 MeV and 1.404 MeV, respectively, yielding an excitation energy of 0.326 MeV for the first  $2^+$  state in the daughter nucleus  $^{144}\text{Er}$ . The  $2^+$  branching ratio is 9.9%. If this were a deformed nucleus, it would imply a deformation of  $\beta_2 \approx 0.18$ , but calculations in the adiabatic limit for these conditions cannot reproduce either the half-life or the branching ratio, for states near the Fermi surface.

This suggests that another approach be tried, namely, to consider the daughter nucleus to be vibrational in nature, rather than permanently deformed. We have modified our coupled-channels formalism<sup>2</sup> to include particle-vibration couplings in the single-particle Hamiltonian, along with the spherical Coulomb, nuclear and spin-orbit terms. The strength  $\alpha_0$  of the coupling to the  $2^+$  state of the daughter nucleus can be related empirically to the excitation energy  $E_x(2^+)$  by the

relation  $\alpha_2^{(0)} = 218/[A\sqrt{E_x(2^+)}]$ . We have used the same nuclear potential parameters that were determined in Ref. [2]. Assuming a total spin of  $11/2^-$  we obtain remarkable agreement with both the total and the partial proton decay widths of  $^{145}\text{Tm}$ .

We have also applied the particle-vibration model to calculate the decay widths  $\Gamma_{\text{th}}$  of other near-spherical proton emitters, with a vibrational coupling strength determined from the  $2^+$  excitation energy when known, or from systematics. The spectroscopic factors, defined as the ratio  $S_{\text{exp}} = \Gamma_{\text{exp}}/\Gamma_{\text{th}}$  of measured and calculated decay widths, are shown by symbols in Fig. V-15 (a) for a number of (odd-Z, odd-A) nuclei. The spectroscopic factors one obtains when the decay widths  $\Gamma_{\text{th}}$  are calculated in a spherical calculation (without any couplings) are shown in (b). Comparing (a) and (b), it is seen that particle-vibration coupling has a significant effect and improves the agreement with the

low-seniority shell model calculations of Ref. [3], which are shown by the solid curves. The results shown in (c) are for a number of (odd-Z, odd-N) nuclei. They were also obtained in the particle-vibration model,

treating the odd neutron as a spectator. Here, too, the agreement with the low-seniority calculation is quite good. This work has been published.<sup>4</sup>

<sup>1</sup>K. Rykaczewski *et al.*, Nucl. Phys. A **682**, 270c (2001)

<sup>2</sup>H. Esbensen and C. N. Davids, Phys. Rev. C **63**, 014315 (2001)

<sup>3</sup>Cary N. Davids *et al.*, Phys. Rev. C **55**, 2255 (1997)

<sup>4</sup>Cary N. Davids and H. Esbensen, Phys. Rev. C **64**, 034317 (2001)

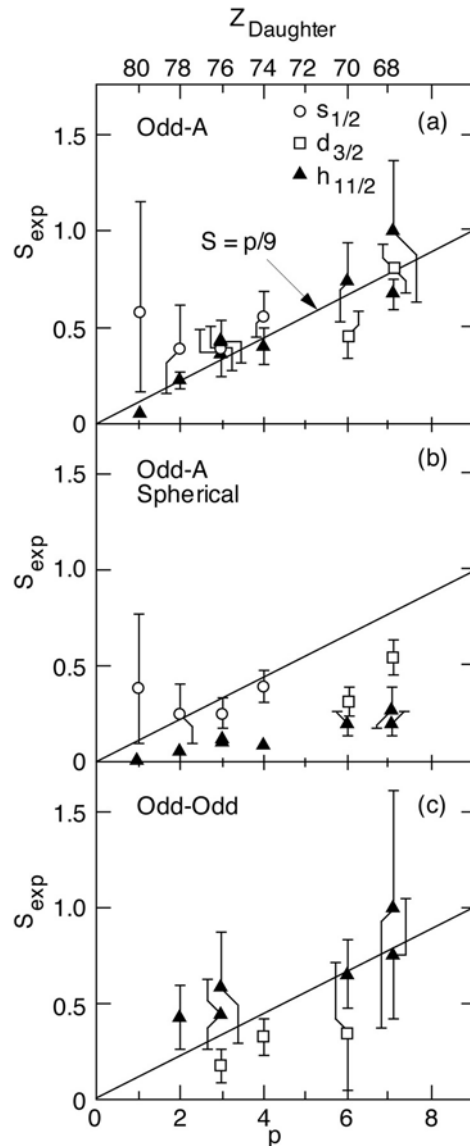


Fig. V-15. Spectroscopic factors of near-spherical proton emitters, as function of the number  $p$  of proton holes below  $Z = 82$ . The solid curves are the predictions of a low-seniority shell model calculation.<sup>3</sup> The symbols in (a) are the values obtained for (odd-Z, odd-A) nuclei and include the effect of particle-vibration coupling. The symbols in (b) are the results for the same set of nuclei obtained without any particle-vibration coupling. The results in (c) are for odd-odd nuclei. They include the effect of particle-vibration coupling and treat the odd neutron as a spectator.

### c.3. Accuracy of the Eikonal Model of Fragmentation Reactions (H. Esbensen and G. F. Bertsch\*)

A convenient model of the nuclear induced breakup of halo nuclei is the eikonal approximation which is well justified at high energies. Since many fragmentation experiments have been performed in the energy range of 20-60 MeV/u, it is of interest to see how accurate the eikonal approximation is in this energy range and at which energy it becomes unreliable. We have tested the eikonal approximation by comparing it to solutions of the time-dependent Schrödinger equation, where we numerically follow the time evolution of the wave function for the relative motion of a halo nucleon and a core nucleus, under the influence of the nuclear field from a target nucleus. We take  $^{11}\text{Be}$  as a typical example and use standard optical potentials to describe the interaction with the target. We have compared the one-neutron removal probabilities that we obtain from the two methods, and also the two separate components from stripping and diffraction dissociation.

We have calculated the breakup probabilities on a  $^{12}\text{C}$  target as function of the beam energy, at a typical impact parameter of 8 fm. We found that the eikonal approximation becomes unreliable below 20 MeV/u. At higher energies, the eikonal breakup probability is

reduced compared to the dynamical calculation by roughly the factor  $1 - E_x/E_{\text{beam}}$ , where  $E_{\text{beam}}$  is the beam energy in MeV/u and  $E_x \approx 4.5$  MeV. The reduction implies that an absolute spectroscopic factor extracted in the eikonal approximation from measurements at 60 MeV/u should be reduced by about 7%.

We have also investigated the longitudinal momentum distribution of neutrons emitted in the breakup. At 10 MeV/u we obtain an asymmetric distribution in the dynamical calculation, whereas the eikonal is symmetric. By decomposing the asymmetric distribution (shown by the solid curve in Fig. V-16) into contributions from low and high final state angular momenta  $l_f$  in the rest frame of  $^{11}\text{Be}$ , we obtained a fairly narrow and symmetric distribution from  $l_f \leq 5$  (long dashed curve). From  $l_f > 5$ , we obtained a very broad distribution centered around the target motion (short dashed curve). The latter component was interpreted as a towing mode, where some of the emitted neutrons are attracted to the target nucleus and follow its motion. This work has been published.<sup>1</sup>

\*Institute for Nuclear Theory, Univ. of Washington

<sup>1</sup>H. Esbensen and G. F. Bertsch, Phys. Rev. C **64**, 014608 (2001)

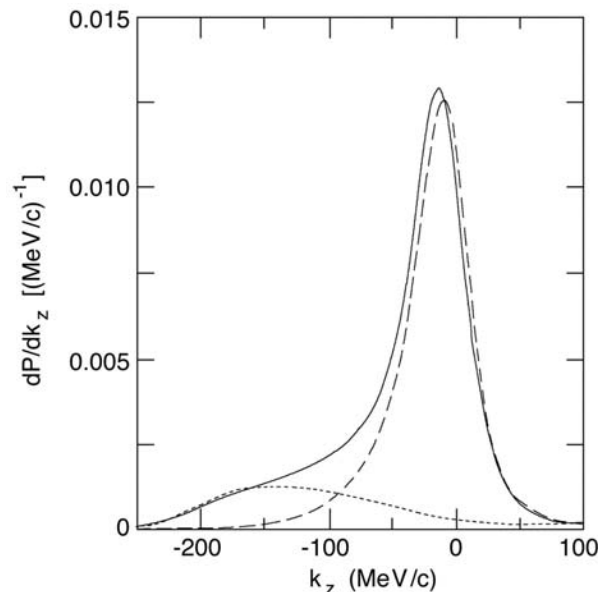


Fig. V-16. Longitudinal momentum distribution of neutrons emitted in the rest frame of  $^{11}\text{Be}$  in reactions with a  $^{12}\text{C}$  target at 10 MeV/u and an impact parameter of 8 fm. The full distribution (solid curve) has been decomposed into two components: from low-angular momenta ( $\leq 5$ , long-dashed curve) and high-angular momenta ( $> 5$ , short dashed curve).

#### c.4. Higher-order Effects in the Two-body Breakup of $^{17}\text{F}$ (H. Esbensen and G. F. Bertsch\*)

Measurements of the Coulomb dissociation of weakly bound proton-rich nuclei (*e.g.*,  $^8\text{B}$ ) are commonly analyzed on the basis of first-order perturbation theory for distant collisions. We have investigated the validity of this approximation by calculating the diffraction dissociation of  $^{17}\text{F}$  to all orders in the Coulomb and nuclear fields from a target nucleus. This is done by assuming a classical Coulomb trajectory for the relative motion of projectile and target and by numerically solving the time-dependent Schrödinger equation for the two-body wave function of the valence proton and the  $^{16}\text{O}$  core, in the time-dependent fields from the target.

We find that the most dominant correction to the first-order Coulomb dissociation is a dynamic polarization effect which to lowest order is proportional to  $Z^3$  of the target charge. This effect is known in atomic stopping theory as the Barkas effect.<sup>1</sup> It causes a reduction in the stopping power of negative charged particles and an enhanced stopping of positive charged particles, compared to first-order perturbation theory (Bethe's formula). The Coulomb dissociation of  $^{17}\text{F}$  has some analogy with the stopping of negative charged particles because the Coulomb fields that are involved in the excitation of the proton state and the electrons in a solid, respectively, are repulsive in both cases. Thus we find a reduction in the Coulomb dissociation probabilities compared to the first-order calculation.

We have extracted the Barkas effect from our dynamical calculations by repeating them for a negative charged target. Denoting the two sets of Coulomb dissociation probabilities by  $P_{\text{CD}}^{(\pm)}$ , with positive and negative target charge, respectively, we define the Barkas factor:  $B = [P^{(+)} - P^{(-)}]/[P^{(+)} + P^{(-)}]$ , and also the ratio of the average compared to first-order perturbation theory ( $P_{\text{pth}}$ ):  $A = [P^{(+)} + P^{(-)}]/[2P_{\text{pth}}]$ . The two factors

we obtain for a  $^{58}\text{Ni}$  target are shown in Fig. V-17 as functions of the impact parameter  $b$ , at beam energies  $E_{\text{beam}} = 10$  (solid points), 20 (squares), and 40 MeV/u (diamonds).

The A-factors, shown in the left panel, approach one at large impact parameters and higher beam energies. At small impact parameters, the A-factors are strongly reduced compared to one. The main reason is that the first-order calculation was performed under the assumption that the projectile and target densities do not overlap during the collision. The reduction is even more dramatic in the Coulomb dissociation of the  $1/2^+$  excited state in  $^{17}\text{F}$ , where it persists out to  $b = 30$  fm.

The solid curves for the B-factors (right panel) show the parameterization

$$B = \frac{CZe^2}{E_{\text{beam}} \sqrt{b^2 + a^2}},$$

where  $C = -1.68$  and  $a = 20$  fm have been adjusted to fit the extracted values. The Z-dependence of this parameterization is consistent with the lowest-order Barkas effect. It was tested by repeating the dynamical calculations for a Pb target and good agreement was found at 40 MeV/u. However, the fit became poor at 10 MeV/u due to the onset of corrections of even higher order than  $Z^3$ .

We also investigated the influence of Coulomb-nuclear interference. It appears from our results that the transition from Coulomb- to nuclear-dominated breakup occurs quite abruptly, with a surprisingly small effect of the Coulomb-nuclear interference at larger impact parameters. This work has been accepted for publication.<sup>2</sup>

\*Institute for Nuclear Theory, Univ. of Washington

<sup>1</sup>W. H. Barkas, N. J. Dyer, and H. H. Heckman, Phys. Rev. Lett. **11**, 26 (1963)

<sup>2</sup>H. Esbensen and G. F. Bertsch, Nucl. Phys. A (in press)

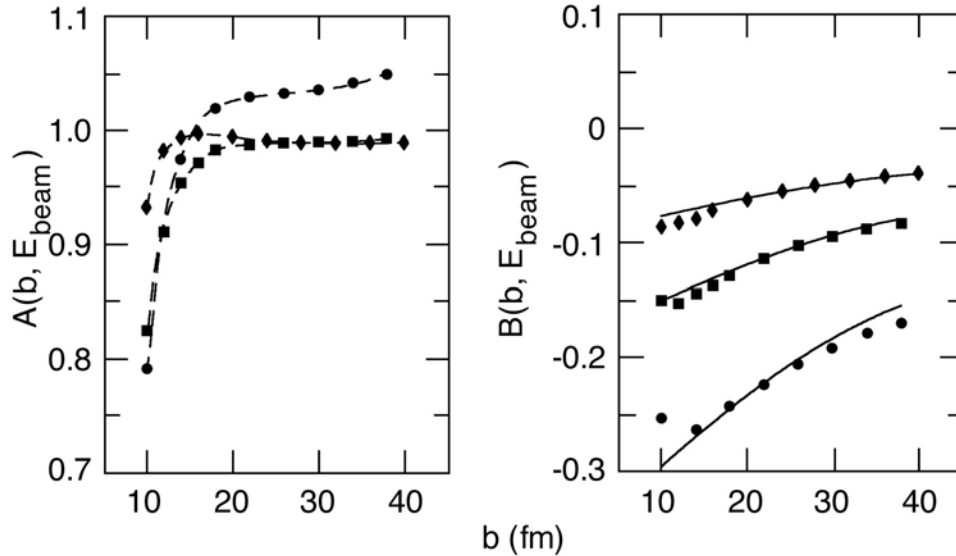


Fig. V-17. The A- and B-factors defined in the text have been extracted from dynamical Coulomb dissociation of  $^{17}\text{F}$  on a  $^{58}\text{Ni}$  target at 10 MeV/u (solid points), 20 (squares), and 40 MeV/u (diamonds). They are shown as functions of the impact parameter  $b$ . The solid curves show the simple parameterization of the B-factor suggested in the text. The dashed curves connect the A-values at fixed beam energy.

### c.5. Many Body Wave Functions (R. R. Chasman)

We are continuing the development of a program for calculating many-body variational wave functions that puts pairing and particle-hole two-body interactions on an equal footing. The variational parameters are calculated with an iteration procedure. The complexity of the wave functions depends only on the number of levels included in the valence space, but does not depend on the number of nucleons in the system. In these wave functions, we conserve particle number and parity strictly; projecting states of good particle number and parity before carrying out the variational calculations. We have added a cranking term to the many-body Hamiltonian and modified the projection procedure to get states of good signature before variation. This allows us to study pairing collapse as a function of angular momentum. We have also extended the program to calculate the spectroscopic factors involved in proton decay. This is useful for studies of nuclides near the proton drip line.

By using residual interaction strengths (*e.g.*, the quadrupole interaction strength or pairing interaction strength) as generator coordinates, one gets many different wave functions; each having a different expectation value for the relevant interaction mode. Such wave functions are particularly useful when one is dealing with a situation in which a configuration interaction treatment is needed. This is particularly true for an adequate treatment of pairing at high spin as well

as for instances in which the single-particle level density is low. Because the same basis states are used in the construction of all of the many-body wave functions, it is possible to easily calculate overlaps and interaction matrix elements for the many-body wave functions obtained from different values of the generator coordinates (which are not in general orthogonal). The valence space can contain a very large number of single-particle basis states, when there are constants of motion that can be used to break the levels up into sub-groups.

Wave functions of this sort become more realistic as the size of each of the sub-groups is increased. To increase this size, we have parallelized our code to run on the SP computer system. We have also modified our codes to handle arbitrary two-body matrix elements. This latter feature allows us to include Coulomb matrix elements easily. Together with J. L. Egido and L. M. Robledo, we have developed subroutines for calculating Gogny interaction matrix elements and Coulomb matrix elements for this many-body code.

In the past year, our major effort has been to extend our many-body code to include neutron-proton pairing interactions, in both the  $T = 0$  and  $T = 1$  modes. Such pairing is expected to be important for nuclides near the  $N = Z$  line.



### c.6. Neutron-Proton Pairing (R. R. Chasman)

In most nuclides, the fermi levels of protons and neutrons are sufficiently different that  $T = 1$  n-n and p-p pairing are the dominant particle-particle residual interaction modes. In nuclides with roughly equal numbers of protons and neutrons, one expects that the  $T = 1$  n-p interaction will also play an important role, as well as the  $T = 0$  n-p interaction. In order to get a good handle on these effects, it is necessary to go beyond the quasi-particle approximation. To get a clear signal of n-p pairing, it is necessary to study not only nuclei along the  $N = Z$  line, but also the nuclides in the vicinity of the  $N = Z$  line. With the advent of a rare isotope accelerator, we anticipate that considerable spectroscopic information will become available on nuclides near the  $N = Z$  line.

We have extended<sup>1</sup> our many-body method to include n-p pairing, with full projection of neutron and proton particle number before doing a variational calculation. We have also found that there is a new quantum number that holds exactly for collective states; *i.e.* those states in which no levels are blocked. This new

quantum number ( $Q$ ) is the number parity of the  $T = 0$  and  $T = 1$  n-p pairs. Fixing the number parity of one n-p mode fixes the other, when the number of neutrons and protons is fixed. This number parity is closely related to the isospin quantum number. The collective states are the ground states for  $N = Z$  nuclides. We project  $Q$  - before doing a variational calculation. By doing calculations that conserve  $Q$ , we find a remarkable multiplicity of degenerate levels in odd-odd nuclides, with  $N = Z \pm 2m$ . Such multiplets are at or near ground for  $m = 1$  or  $2$ . The form of our variational wave function includes an explicit amplitude for 'alpha like' correlations in each level as well as the usual amplitudes for n-n, p-p and n-p pairs. In Fig. V-18, we compare the amplitude for one of the two particle modes [ $U(1,k)$ ] in a given level and four particles in that level [ $U(5,k)$ ] as a function of the level number, in a model  $N = Z$  even-even nucleus ( $^{60}\text{EE}$ ). Level 15 is the fermi level. The insert in the figure shows the level degeneracies in odd-odd nuclides ( $^{62}\text{OO}$ ,  $^{64}\text{OO}$ ,  $^{66}\text{OO}$ ) near the  $N = Z$  line.

<sup>1</sup>R. R. Chasman, Phys. Lett. B **524**, 81 (2002)

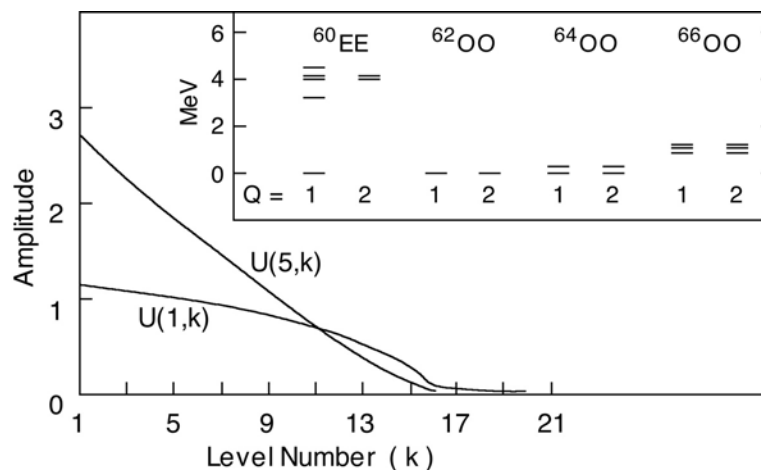


Fig. V-18. Ground state amplitudes in  $^{60}\text{EE}$ . Low lying states in  $^{60}\text{EE}$ ,  $^{62}\text{OO}$ ,  $^{64}\text{OO}$  and  $^{66}\text{OO}$  are shown in the insert, illustrating the extra degeneracies arising from multiple pairing modes.

### c.7. Very Extended Shapes in Nuclei (R.R. Chasman)

In the past few years, large computer resources have become available on the massively parallel processor IBM SP system at Argonne, in addition to the resources provided by NERSC. We have parallelized the code used to calculate single-particle spectra to exploit the SP system and have devoted a large part of our efforts to calculating energy surfaces in a four dimensional shape space that includes reflection asymmetric shapes. We study the nuclear energy surfaces as a function of mass, charge, shape and angular momentum, using the Strutinsky method. In this approach, one makes quantum corrections to a smooth liquid drop behavior using the calculated single particle energy levels. In earlier studies we found that it is often not sufficient to use only quadrupole and hexadecapole deformations to describe very extended reflection symmetric nuclear shapes. When we added a necking degree of freedom we found previously unknown minima. These minima are characterized by very extended capsule shaped nuclei with axis ratios of 2.2:1 in the  $A = 180$  mass region. We have now added octupole deformation to this shape space. The inclusion of these two degrees of freedom to our shape space substantially increases our ability to describe nuclear shapes compared to a typical shape space consisting only of quadrupole and hexadecapole deformations. As parity is no longer a good quantum number when octupole deformation is included, the size of the matrices that we diagonalize is doubled. In a typical calculation, we diagonalize matrices that are  $600 \times 600$ . Several thousand such diagonalizations are needed to determine energy surfaces.

There remains a need to test calculated fission barriers and to generally understand nuclear properties at the

<sup>1</sup>R. R. Chasman, Workshop on the Science for an Advanced ISOL Facility, Columbus, OH, Jul. 31-Aug. 1, 1997, p. 69

<sup>2</sup>R. R. Chasman, Phys. Rev. C **64**, 024311 (2001)

### c.8. E1 Transition Probabilities Between Superdeformed States (R. R. Chasman)

Recent experimental studies have found E1 transition probabilities between superdeformed states on the order of 1 milli-Weiskopf unit (mWu), and this observation has given rise to speculation that such transitions are evidence for octupole vibrational states in superdeformed minima. It was assumed that E1 transition probabilities of this magnitude are too large to be due to single-particle transitions.

highest spins. Using the four-dimensional deformation space described above, we have analyzed the high spin energy surfaces of the  $N = 86$  isotones going from Sn ( $Z=50$ ) to Dy ( $Z=66$ ). There is a high spin superdeformed minimum in all of these nuclides ( $\sim 1.85:1$  axis ratio) that becomes yrast at high spin. These shapes are well known experimentally in the Dy region.

We find that as the proton number decreases from  $Z = 66$  to  $Z = 50$ , the fission barrier increases by roughly 10 MeV at a given angular momentum. The superdeformed minimum associated with  $N = 86$  is present for both Sn and Dy. This result suggests that we can extend the study of nuclear properties at extreme deformations to a new regime of angular momenta, with the availability of radioactive nuclear beam facilities. A preliminary version of this work has been published.<sup>1</sup>

We have extended our high spin Strutinsky calculations<sup>2</sup> to nuclei in the  $A = 100$  mass region. Many of the very extended minima that we find will be accessible with projectiles produced at an exotic beam facility. However, our calculations show very extended minima in nuclides in the vicinity of  $^{108}\text{Cd}$  that are accessible using existing facilities. Recent experiments, inspired by these calculations, show a superdeformed rotational band in  $^{108}\text{Cd}$ . Our results for the  $A = 100$  mass region have recently been published.

We are analyzing nuclides in the region  $70 < A < 100$ , searching for nuclides with well-deformed shapes.

We have calculated single-particle E1 transition rates for low-lying orbitals in the  $A = 190$  and  $A = 150$  regions of superdeformation. We find that there are indeed single-particle E1 transition matrix elements, for neutron orbitals near  $N = 110$ , that are sufficiently large to account for the observed transitions. Additionally, we have found other cases ( $Z < 80$ ) in which equally large E1 transition probabilities between superdeformed levels might be found.

### c.9. Single Particle States in the Heaviest Elements (I. Ahmad and R. R. Chasman)

The search for superheavy elements has been a major theme of nuclear structure research for the past forty years. Theoretical predictions of the stability of superheavy elements depend crucially on the single-particle energy level spacings in the vicinity of 114 protons and 184 neutrons. Our approach<sup>1,2,3,4</sup> is to learn as much as possible about these levels from spectroscopic studies of nuclides in the  $A = 250$  region. This is possible because there are members of the relevant spherical multiplets that drop rapidly in energy with increasing deformation, and are fairly close to the ground state in the strongly deformed nuclides near  $A =$

250. Our analysis<sup>4</sup> of excited states in  $^{251}\text{Cf}$  populated in the alpha decay of  $^{255}\text{Fm}$  allows us to characterize several single-particle and vibrational states beyond the  $N = 162$  deformed gap. Another effect of the  $N = 162$  gap would be on alpha decay properties of nuclides having 163 neutrons. Using the potential parameters derived from our studies, we find that there are two favored alpha decays that might be observed in  $^{273}\text{110}$ , having an energy difference of 1.7 MeV. The lower energy transition is the favored alpha decay from the ground state of  $^{273}\text{110}$  and the higher energy one is the favored transition to the ground state of  $^{269}\text{Hs}$ .

<sup>1</sup>I. Ahmad *et al.*, Nucl. Phys. **646**, 175 (1999)

<sup>2</sup>R. R. Chasman and I. Ahmad, Phys. Lett. **B392**, 255 (1997)

<sup>3</sup>I. Ahmad, R. R. Chasman, and P.R. Fields, Phys. Rev. C **61**, 044301 (2000)

<sup>4</sup>I. Ahmad *et al.*, Phys. Rev. C **62**, 064302 (2000)

### c.10. Studies of Nuclear Energy Surfaces (R. R. Chasman, J. L. Egido,\* and L. M. Robledo\*)

This collaborative research program<sup>1,2,3</sup> is focused on the study of nuclear energy surfaces, with an emphasis on very deformed shapes using several complementary methods: 1) the Strutinsky method, 2) Hartree-Fock-Bogoliubov (HFB) calculations using the Gogny interaction, and 3) many-body variational wave functions that we have described above. Our strategy is to identify phenomena and nuclides of interest using the Strutinsky method and to study the most interesting cases with the HFB and many-body (MB) approaches. The two latter approaches include many-body effects and describe these features more accurately.

The great advantage of the Strutinsky method is that one can study the energy surfaces of many nuclides ( $\sim 300$ ) with a single set of calculations. Although the HFB and many-body calculations MB calculations are quite time consuming relative to the Strutinsky calculations, they have many advantages. For the studies of the Pb isotopes described below, they have the advantage that configuration interaction effects can easily be incorporated into the calculations. In this way, we deal directly with the issue of insuring the orthogonality of states that have the same spins and parities.

The neutron deficient nuclides ( $N < 110$ ) in the Pb region have states that are characterized by three distinct shapes; spherical, prolate and oblate. In the oblate and prolate minima, there are low-lying single particle states derived from spherical states on both sides of the  $Z = 82$  single particle gap. Although this gap is roughly 4 MeV, there are states within a few hundred keV of ground in the neutron deficient Tl( $Z=81$ ) and Bi( $Z=83$ ) isotopes that would be at  $\sim 4$  MeV excitation, in the simplest single particle picture. Our approach is to determine the nuclear wave function as a function of quadrupole moment, letting other deformation modes (*e.g.* P4 and P6) vary freely. Using both the HFB and MB methods, we find<sup>3</sup> three low-lying states in the isotopes  $^{190,188,186,184}\text{Pb}$ . There is remarkably good agreement between the HFB and MB results. In both the HFB and MB calculations, the three separate low-energy  $0^+$  states persist after the configuration interaction is taken into account. These are the first calculations that give a  $0^+$  oblate state in  $^{186}\text{Pb}$ , in agreement with the experimental observation of two  $0^+$  excited states in this nuclide. Both calculations also predict an as yet unobserved  $0^+$  state in  $^{184}\text{Pb}$ . Investigations are under way to search for this state.

\*Universidad Autonoma de Madrid

<sup>1</sup>R. R. Chasman and L. M. Robledo, Phys. Lett. **B351**, 18 (1995)

<sup>2</sup>J. L. Egido, L. M. Robledo, and R. R. Chasman, Phys. Lett. **B393**, 13 (1997)

<sup>3</sup>R. R. Chasman, J. L. Egido and L. M. Robledo, Phys. Lett. **B513**, 513 (2001)

**c.11. Probing the Gateway to Superheavy Nuclei in Cranked Relativistic Hartree-Bogoliubov Theory** (A. V. Afanasjev, T. L. Khoo, I. Ahmad, S. Frauendorf,\* and G. A. Lalazissis†)

The cranked relativistic Hartree-Bogoliubov theory<sup>1</sup> (CRHB), including approximate particle number projection through the Lipkin-Nogami method and the Gogny force in the particle-particle pairing channel, has been applied for a systematic study of the nuclei around <sup>254</sup>No.<sup>2</sup> These are the heaviest elements with a large body of spectroscopic data for testing the reliability of mean-field theory predictions for superheavy nuclei. The deformation, rotational response, pair correlations, quasiparticle spectra, nucleon separation energies and shell structure of these nuclei have been extensively studied with different RMF forces.

While the deformation properties are well reproduced, the calculations reveal that an accurate description of other observables requires better effective forces both in the particle-hole and particle-particle channels. The calculated moments of inertia show only small sensitivity to the RMF force and thus to the details of the single-particle structure. In contrast to previous studies, where the moments of inertia in lighter systems<sup>1,3</sup> are well reproduced, good agreement in the heaviest nuclei can be obtained only with a decrease ( $\approx 12\%$ ) of the strength of the D1S Gogny force in the pairing channel.

The CRHB theory has been extended for a detailed description of quasi-particle states in odd and odd-odd nuclei. For the first time, the blocking procedure in such nuclei has been performed fully self-consistently, with effects of the breaking of time-reversal symmetry (nuclear magnetism) taken into account. Analysis of quasi-particle spectra in odd <sup>249,251</sup>Cf and <sup>249</sup>Bk nuclei with the NL1 and NL3 forces (see Fig. V-19 for an example) suggests that the energies of most of the spherical orbitals, from which active deformed states of

these nuclei emerge, are described with an accuracy better than 0.5 MeV. However, for a few subshells the discrepancies reach 1.0 MeV. Considering that the RMF forces were fitted only to bulk properties of spherical nuclei without considering single-particle energies, this level of agreement is impressive. However, in very heavy systems, where the level density is high, the accuracy is not sufficient for reliable predictions of the location of deformed shell gaps, which are small ( $\approx 1$  MeV).

The results of the present investigation have a number of implications for the study of superheavy nuclei. The NL-SH and NL-RA1 forces do not provide satisfactory descriptions of the single-particle energies: the deviation between experiment and theory in the  $A \sim 250$  mass region reach 2 MeV for some spherical subshells. Thus their application to superheavy nuclei is not recommended. The extrapolation of the results for quasiparticle states obtained in the  $A \sim 250$  mass region suggest that the NL1, NL3 and NL-Z forces provide reasonable descriptions of most of the states in the vicinity of the  $Z = 120$  and  $N = 172$  spherical shell gaps. These are magic gaps in most parameterizations of the RMF theory. However, it is not possible to estimate the accuracy of the description of some low- $j$  states, such as  $\nu 3d_{3/2}$ ,  $\nu 4s_{1/2}$  and  $\pi 3p_{3/2}$ ,  $\pi 3p_{1/2}$ , which are located near these gaps by studying lighter deformed nuclei. Thus the particle numbers corresponding to magic gaps in superheavy nuclei still remain an open question. In addition, the study of a number of effects in superheavy nuclei, such as pairing and the importance of self-consistency, is in progress. A paper on this work is being prepared.

\*University of Notre Dame, †Aristotle University, Thessaloniki, Greece

<sup>1</sup>A. V. Afanasjev, P. Ring and J. Konig, Nucl. Phys. A **676**, 196 (2000)

<sup>2</sup>P. Reiter *et al.*, Phys. Rev. Lett. **82**, 509 (1999)

<sup>3</sup>A. V. Afanasjev *et al.*, Phys. Rev. C **62**, 054306 (2000)

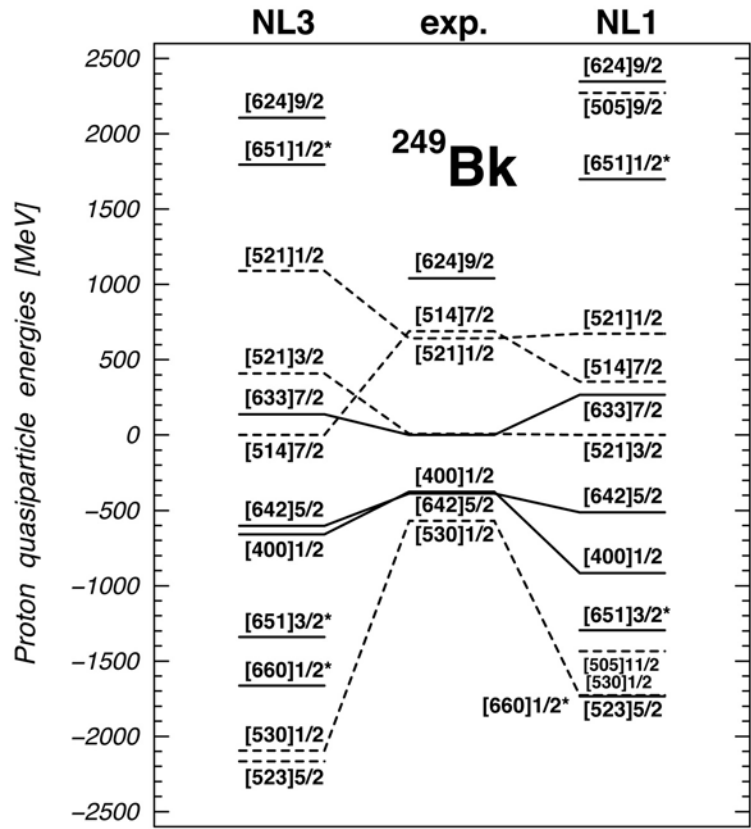


Fig. V-19. Experimental and theoretical quasiparticle energies of neutron states in  $^{249}\text{Bk}$ . Positive and negative energies are used for particle and hole states, respectively. Solid and dashed lines are used for positive and negative parity states, respectively. The symbols 'NL3' and 'NL1' indicate the RMF force used in calculations.

#### D. ATOMIC THEORY AND FUNDAMENTAL QUANTUM MECHANICS

In addition to research on hadronic and nuclear physics, we also conduct research in atomic physics, neutron physics, and quantum computing.

Recent work in atomic physics includes the studies of interactions of high-energy photons with matter, in support of experiments performed at Argonne's Advanced Photon Source (APS). Theoretical studies are being conducted on the physics of the Photoeffect and Compton scattering by bound electrons, focusing on topics selected in view of basic importance, timeliness, and potential in applications. We also produced a review on "Electron collision cross sections of atoms" for inclusion in a volume on "Atomic Collisions" in the Landolt-Börnstein Numerical Data and Functional Relationships series.

Recent theoretical work in support of a new experiment to measure the neutron electric-dipole moment has been focusing on experimental challenges resulting from the time spent by the neutron inside a silicon crystal in the Bragg reflection process. Additionally, a new investigation of the basis of the spin-statistics theorem in nonrelativistic quantum mechanics, following the geometrical approach of Berry and Robbins, has shown that spin-zero particles must obey boson statistics without the usual assumptions of relativistic local field theory.

Work in areas related to quantum computing continued by extending, to integers and rational numbers, earlier work on the conditions that states of physical systems must satisfy in order to represent natural numbers. Emphasis was placed on the condition of efficient physical implementation of the basic arithmetic operations on the states whose properties are given by the appropriate axioms for the different types of numbers. The relation between efficient implementation and the product state representation of numbers was also studied.

Work was also begun on a framework for developing a coherent theory of mathematics and physics together. This work is partly based on the universal applicability of quantum mechanics, or a suitable generalization, and earlier work on an example of the use of mathematical logical concepts in quantum mechanics. In essence the idea is to integrate mathematical logical concepts with quantum mechanics. A basic and possibly defining requirement for a coherent theory was described and discussed, along with other aspects.

### d.1. Interactions of Photons with Matter (M. Inokuti and D. Y. Smith\*)

In support of experiments in atomic and condensed-matter physics with the use of synchrotron radiation, theoretical studies are being conducted on the physics of photo-absorption and Compton scattering, focusing on topics selected in view of basic importance, timeliness, and potential applications.

One theme of long-term studies has been the use of dispersion relations and sum rules for indices of response of matter over the entire range of photon

energies. A comprehensive analysis of optical data on silicon<sup>1</sup> is in progress, and a new expression for the refractive index in a region of near transparency<sup>2</sup> is applied to graphite, silicon, and germanium.

A sum rule for the absorption strength originally due to Vinti<sup>3</sup> is applied to color centers in alkali halides to derive the spatial extent of the electronic structure of the color centers.<sup>4</sup>

\*University of Vermont

<sup>1</sup>D. Y. Smith, M. Inokuti, and W. Karsten, *Physics Essays* **13**, 465 (2000)

<sup>2</sup>D. Y. Smith and M. Inokuti, *J. Phys. C: Condensed Matter* **13**, 3883 (2001)

<sup>3</sup>J. P. Vinti, *Phys. Rev.* **41**, 432 (1932)

<sup>4</sup>D. Y. Smith and M. Inokuti, *Radiat. Effects Defects Solids* **155**, 43 (2001)

### d.2. Interactions of Charged Particles with Matter (M. Inokuti)

Stopping power, the total yield of ionization, and its statistical fluctuations are examples of quantities describing the penetration of charged particles through matter and are important to applications such as the detection of particles and the analysis of their charges and kinetic energies. The understanding of those quantities in terms of individual collisions and associated cross sections remains a major challenge and is the goal of our continuing effort. A review<sup>1</sup> of cross sections for electron collision with atoms has been published.

Unpublished materials left by R. L. Platzman (1918-

73), a pioneer of radiation physics and chemistry and a former Argonne staff member (1958-65), are studied<sup>2</sup> and being prepared for an archive in the Joseph Regenstein Library of the University of Chicago.

An essay<sup>3</sup> on the role of physics in radiation sciences was written in commemoration of the 50<sup>th</sup> anniversary of the Radiation Research Society. Extensive work for the International Commission on Radiation Units and Measurements (ICRU) continues on the editing of its reports and on physical data such as stopping powers and various interaction cross sections.

<sup>1</sup>M. Inokuti, in *Landolt-Börnstein Numerical Data and Functional Relationships in Science and Technology*, Vol. 1/17, ed. Y. Itikawa (Springer-Verlag, Berlin 2000), pp. 2.1-2.34

<sup>2</sup>M. Inokuti, *Radiat. Phys. Chem.* **60**, 283 (2000)

<sup>3</sup>M. Inokuti and S. M. Seltzer, *Radiat. Res.*, in press

### d.3. On the Connection Between Spin and Statistics in Quantum Mechanics (Murray Peshkin)

The connection between spin and statistics has traditionally been thought to depend upon the assumptions of local relativistic quantum field theory or at least upon the existence of antiparticles. However, Michael Berry and Jonathan Robbins recently identified it as a geometrical feature of nonrelativistic quantum mechanics. The key physical feature of their geometrical approach is taking seriously the indistinguishability of identical particles. Thus for two spinless particles, the dynamical variables are unordered coordinate pairs  $\{\mathbf{r}_1, \mathbf{r}_2\}$ , and similarly for the momenta. For particles with spin, the spin variables

must also be included. That  $\{\mathbf{r}_1, \mathbf{r}_2\}$  is the same point in the configuration space as  $\{\mathbf{r}_2, \mathbf{r}_1\}$  changes the topology from that in the case of distinguishable particles, and that has consequences for quantum mechanics. Berry and Robbins showed under reasonable mathematical assumptions that this leads to integer-spin particles having symmetric statistics and half-integer-spin particles having antisymmetric statistics. They also found other mathematical assumptions that could violate that result, but they are in some way weird and possibly do not apply to real physics.

I have implemented the Berry-Robbins approach in a somewhat different way in the simplest case, that of two spinless particles, and found that I can unambiguously exclude antisymmetric statistics in that case. I follow Berry and Robbins in assuming that  $\{\mathbf{r}_1, \mathbf{r}_2\} = \{\mathbf{r}_2, \mathbf{r}_1\}$  and in requiring that the wave function must be continuous in the particles' coordinates because of the second derivative in the Schrödinger equation. Those conditions are sufficient to eliminate odd values of the angular momentum of the relative

motion of the two particles. The present approach has, in addition to its apparently stronger conclusion, the advantage that it illuminates directly the connection between the topology and orbital angular momentum in a very elementary way. In contrast to the Berry-Robbins work, it has the disadvantage that it does not directly demonstrate the relation between the statistics and the geometrical Berry phase. Whether my approach adds anything to Berry and Robbins in the case of spinning particles is not yet clear.

#### d.4. A Virial Theorem for Nuclear Deformation (Murray Peshkin)

Calculations of nuclear deformation frequently start by minimizing the ground-state energy of the nucleus with respect to a "volume preserving" deformation of some collective potential  $V$ . Specifically, one introduces a deformed potential  $V_{abc}(x,y,z) = V(ax,by,cz)$  with the constraint that  $abc = 1$  and minimizes the ground-state energy to determine the deformation parameters  $a,b,c$ . That long-used prescription has always been mysterious because no variation principle supports it and no reasonable nuclear structure model suggests it in any direct way. The nearest thing to a physical justification was given many years ago by Bohr and Mottelson, who observed that for a shell model with harmonic oscillator potential and no inter-particle or spin-orbit interactions, the minimum-energy assumption leads to a state whose kinetic energy tensor in the rotating system has spherical symmetry, *i.e.*  $\langle \sum_n p_i^n p_j^n \rangle = T \delta_{ij}$ , where  $n$

labels the particles and  $i,j$  label the three axes. That condition suggests something akin to irrotational flow in the rotating system, which seems not unreasonable for the ground state.

I have shown that a simple virial theorem relates the minimum-energy condition to the spherical kinetic energy tensor for any shell-model potential, not just for the harmonic oscillator. Moreover, that relation remains valid in the presence of residual interactions  $V_{ij}(\mathbf{r}_i, \mathbf{r}_j)$  between the nucleons, but only if the residual interactions are deformed in the same way as the collective potential. It is also valid in the presence of momentum-dependent potentials such as the spin-orbit interaction, but only if the spatial variables are scaled as in the collective potential and the momenta are scaled inversely so that  $p_x \rightarrow p_x/a$ , and similarly for  $p_y$  and  $p_z$ .

#### d.5. The Representation of Numbers in Quantum Mechanics (P. Benioff)

Earlier work on modular arithmetic of  $k$ -ary representations of length  $L$  of the natural numbers in quantum mechanics was extended to  $k$ -ary representations of all natural numbers, and to integers and rational numbers<sup>1</sup>. Since the length  $L$  is indeterminate, representations of states and operators using creation and annihilation operators for bosons and fermions are defined. Emphasis is on definitions and properties of operators corresponding to the basic operations whose properties are given by the axioms for each type of number. The importance of the requirement of efficient implementability for physical models of the axioms is emphasized. This condition

requires the use of successor operations for each value of  $j$ , corresponding to addition of  $k^{j-1}$  if  $j > 0$  and (for rational numbers)  $k^j$  if  $j < 0$ . It follows from the efficient implementability of these successors, which are used in all computers, that implementation of the addition and multiplication operators, which are defined in terms of iterations of the successors, should be efficient. Implementation of definitions of the addition and multiplication operators based on the successor for  $j = 1$  only, which is the only successor defined in the usual axioms of arithmetic, are not efficient.

<sup>1</sup>Paul Benioff, to appear in special issue of the journal *Algorithmica*



### d.6. Efficient Implementation and the Product State Representation of Numbers (P. Benioff)

Work on the relation between the requirement of efficient implementability and the product state representation of numbers was carried out and completed<sup>1</sup>. In this work numbers are defined to be any collection of objects with associated operations and properties that satisfy the axioms of number theory or arithmetic. Product state representations are representations by strings of  $k$  digits or  $k$  dimensional qubits in quantum mechanics for any  $k \geq 2$ . Efficient implementability (EI), which is a basic requirement on any physical model of the numbers, means that the basic arithmetic operations, which are those described by the axioms of arithmetic (successor, plus, and times), are physically implementable and the space-time and thermodynamic resources needed to

carry out the implementations are polynomial in the logarithm of the range of numbers considered (*i.e.*, polynomial in  $\log N$  if the numbers 0 to  $N$  are represented.). Different models of numbers are described, including extremely entangled representations, to show that both EI and the product state representation are not required by the axioms nor do they imply the properties stated by the axioms. The relation between EI and the product state representation is examined. It is seen that the condition of a product state representation does not imply EI. The converse implication, EI does not imply a product state representation, seems reasonable, but it is an open question.

<sup>1</sup>Paul Benioff, Phys. Rev. A **64**, 052310 (2001)

### d.7. Towards a Coherent Theory of Mathematics and Physics (P. Benioff)

Work was begun on describing a framework for developing a coherent theory of mathematics and physics together<sup>1</sup>. This work is partly motivated by the observation that in spite of a close connection, physics and mathematics as presently developed do not take account of any close connection at a foundational level. Also any universally applicable physical theory, by including in its domain observers using mathematics to validate the theory, must describe in some sense its own validation. The main and possibly defining characteristic of such a theory is discussed: the theory must be valid and sufficiently complete and it must describe its own validity and sufficient completeness to the maximum extent possible. Definitions of validity and completeness are based on those used in mathematical logic. The requirement of universal applicability for the theory at least means that it must include the description of intelligent systems and their dynamics in validating a theory. The close connection

between such a theory and the universe is supported by the observation that the reality status of very small or very large cosmological physical systems is more indirect in that it depends on more intervening layers of theory and experiment than for moderate sized systems. This suggests that the basic properties of the physical universe are entwined with and emerge from such a theory. In this case the basic properties may not have an *a priori* status independent of a theoretical description of them. Other aspects of a coherent theory include the observation that language is physical. All symbols and words of any language necessarily have physical representations as states of physical systems that are in the domain of a coherent theory. This is an important property not enjoyed by any purely mathematical theory and may have some important consequences.

<sup>1</sup>Presented at 1<sup>st</sup> Brazilian Symposium on the Philosophy of Nature, Rio de Janeiro, Aug. 24-27, 2001, to appear in symposium proceedings

**d.8. Cyclic Quantum Gate Networks (Paul Benioff and Peter Cabaay\*)**

We are also studying properties of very simple examples of cyclic networks of quantum gates. This work is based on the fact that studies so far have been limited to noncyclic networks of quantum gates as these have been shown sufficient to describe quantum computation. Cyclic networks would be quite useful in studies of quantum control and would be an essential component of any mobile quantum system such as a quantum robot.<sup>1</sup>

We are theoretically exploring the properties of the simplest nontrivial example, and some extensions thereof, of a cyclic network of two qubits interacting through quantum gates. Quantum gates are two qubit interactions with one qubit functioning as the control system. The states of this qubit determine whether a unitary operation on the other qubit is active or is inactive.

This work will provide the bulk of a Ph.D. thesis that is expected to be completed in the spring of 2002.<sup>2</sup>

---

\*ANL and University of Michigan

<sup>1</sup>Paul Benioff, Phys. Rev. A **58**, 893-904, (1998)

<sup>2</sup>Peter Cabaay, Ph.D. Thesis, University of Michigan, in preparation

## E. OTHER ACTIVITIES

### e.1. Theory Workshop on Rare Isotope Physics (R. Chasman and H. Esbensen)

We organized a Theory Institute, which was held June 25-29, 2001, in the Physics Division. The emphasis of the workshop was the development of numerical techniques and new theoretical approaches that can be used in nuclear structure studies of relevance to RIA. Among the subjects discussed were proton emission

from nuclei beyond the proton drip-line, the structure of quasi-bound states, halo nuclei, pairing near the neutron drip-line, and proton-neutron pairing in  $N=Z$  nuclei. The workshop was attended by some 20 theorists from outside the division, as well as by theorists and experimentalists from within the division.

### e.2. 14<sup>th</sup> Annual Midwest Nuclear Theory Get-Together (C. D. Roberts)

The Theory Group hosted the Fourteenth Annual Midwest Nuclear Theory Get-Together on October 5<sup>th</sup> and 6<sup>th</sup>, 2001. Nuclear theorists from a number of Midwest universities get together every fall to find out what different people and groups in the region are working on. The organizational duties rotate among the participants, but Argonne has become the regular meeting place by virtue of its facilities and central location. The organizer for 2001 was Pawel Danielewicz of Michigan State University. The meeting provides a good chance for students to broaden their horizons and get some practical speaking experience in a friendly atmosphere. The format is very

informal, with an agenda of talks being volunteered at the beginning of the meeting. This year we set a record for the largest attendance ever: 37 faculty, postdocs and students from thirteen different universities and colleges in Illinois, Indiana, Iowa, Michigan, Missouri, and Ohio, along with the Argonne staff. Some 30 presentations were made over Friday afternoon and Saturday morning. Topics included relativistic quantum mechanics, gauge and effective field theories, QCD, quantum Monte Carlo methods, nuclear pairing, no-core shell model, relativistic heavy-ion collisions, and neutron matter. A good time was had by all.

